Toward a better representation of Soil evaporation in ORCHIDEE model:
state and pathways of improvement

Ardalan Tootchi
ardalan.tootchi@gmail.com

Internship report submitted to:

Ecole Polytechnique

In partial fulfillment for the award of the degree of

MASTER 2 (MSc.)
in "Water, Air, Pollution and Energy"

September 2015

1. TABLE OF CONTENTS

List of Tables

List of Figures

List of Symbols

Symbol	Name and Definition	Unit
D_0	Molecular diffusion coefficient of water vapor in the air	$m^2.s^{-1}$
θ_{sat}	Volumetric water content at saturation	Ratio; non dimensional
θ_r	Volumetric residual soil water content	Ratio; non dimensional
θ_i	Initial (uniform) water content at the start of the second stage of evaporation	Ratio; non dimensional
θ_1	Volumetric water content of the topsoil layer	Ratio; non dimensional
θ_c	Volumetric critical water content	Ratio; non dimensional
θ_0	Volumetric air dry water content	Ratio; non dimensional
θ_{ice}	Volumetric ice water content	Ratio; non dimensional
θ_{liquid}	Volumetric liquid water content	Ratio; non dimensional
r_{litter}	Litter layer resistance	$s.m^{-1}$
r_l	Liquid water flow resistance of the soil	$s.m^{-1}$
r_a	Aerodynamic resistance of the boundary layer and the standard measurement level	$s.m^{-1}$
r_v	Vapor flow resistance of the soil	$s.m^{-1}$
u_*	Friction velocity	$m.s^{-1}$
$q_s(T)$	Specific humidity of saturated air at T (temperature)	Ratio; non dimensional
q_{air}	Specific humidity of air at a standard level of measurement	Ratio; non dimensional
q_{av}	Specific humidity at the vegetation artificial level	Ratio; non dimensional
E_{pot}	Potential evaporation from soil	$kg.m^{-2}.s^{-1}$
E_{soil}	Actual evaporation from soil	$kg.m^{-2}.s^{-1}$
U_{av}	Wind speed at the artificial vegetation level	$m.s^{-1}$
T_s	Surface temperature	$^\circ K$
h_u	Relative humidity at the surface	Ratio; non dimensional
K	Hydraulic conductivity of top layer	$m.s^{-1}$
ρ_a	Air density at surface layer	$kg.m^{-3}$
ρ_l	Liquid water density	$kg.m^{-3}$
Δz_1	Thickness of the top soil control volume	m
ε	Air filled porosity	Ratio; non dimensional
D_g	Water vapor diffusivity in soil	$m^2.s^{-1}$
K_v	Water vapor conductance	$m.s^{-1}$
δ	Thickness of external diffusive layer	m
K_{vr}	Relative vapor conductance	Ratio; non dimensional

1 Introduction

This is a report summarizing the research done on the improvement of bare soil evaporation presentation in IPSL's Land Surface Model, ORCHIDEE (ORganizing Carbon and Hydrology in Dynamic EcosystEms, http://orchidee.ipsl.jussieu.fr). In Land Surface Models several procedures are embedded to account for different components of latent heat flux exchange and also energy fluxes which are usually simplified forms of complex-nonlinear relationships.

One of the simplest forms of latent heat exchange between land and atmosphere is bare soil evaporation. This component is more important when it comes to agricultural lands or areas with patchy vegetation where soil is exposed to radiation without any obstacle in between. In hydrologic and land surface models, simplified parametrization is used to skip complex and non-linear physics of this phenomenon (Jefferson & Maxwell, 2015). Evaporation from soil is usually difficult to compute due to the numerous input variables which are difficult to obtain accurately. A great deal of effort has been put into validation of bare soil evaporations recently [Lawrence et al, 2007; Blyth et al, 2010; Jefferson &Maxwell, 2015].

Evapotranspiration (ET) from a drying soil usually happens in 3 stages. During the first stage, where soil evaporation is governed by atmospheric demand, the only limitation is the available energy in the upper layer of the soil and the vapor gradient between the soil and air (Brutsaert, 2014). Over the first stage, evaporation from soil is equal to the atmospheric demand. Within the next two stages, soil evaporation is primarily a function soil water content, hydraulic properties of the soil to provide water to the surface and temperature gradient.

Evaporation from the land surface is a major component of the global water cycle (Blyth et al, 2010). Evapotranspiration transfers water from plants and soil to the atmosphere and influences water resources and runoff (Blyth et al, 2010). Global and regional scale partitioning of ET is not accurately known since large-scale observations of ET, let alone its partitioning, are simply not available (Lawrence et al, 2007). Two studies by Choudhury (1998) and Dirmeyer (2005) suggest reasonable partitioning between Transpiration (E_t), Soil evaporation (E_s) and canopy evaporation (E_c). These values range between 52-48 % forE_t, 28-36% for E_s and 16-20% for E_c, for different climates, vegetation types and land-uses. It is worth noting that usually surface flux models are only as accurate as the measurements used to validate them (Twine et al, 2000), and one of the first steps in assessing different evaporation component partitioning is to accept uncertainties in models.

This issue has been discussed in a couple of papers, mostly for CLM (Community Land Model) [Lawrence et al, 2007; Stockli et al, 2008; Sakaguchi & Zeng, 2009], JULES (Hadley Center land surface model- Join U.K. Land Environment Simulator) [Blyth et al, 2011; Blyth et al, 2010] where they have faced the same issue of unreasonable latent heat flux components partitioning. Overestimation of bare soil evaporation is in contrast with available observation and studies. Few available observations and most current land surface schemes indicate that transpiration is the dominant component of evapotranspiration on the global scale, followed by soil evaporation and canopy evaporation [Lawrence et al, 2007; Miralles et al, 2011].

Based on recent study (Miralles et al, 2011) using remote sensed data and simulation, the total amount of soil surface evaporation contributes only about 7% of the total. Although in sparsely vegetated areas, it is the sole contribution. For instance in Sahel, the proportion of rainfall lost through soil surface evaporation is 28%, which is about 42% of total evaporative loss (Wallace & Holwill, 1997). Several methods exist for evaporation measurement; from chamber measurements and Bowen ration systems to using microlysimeters. However most of these methods either don't give good temporal resolution or are not widely used.

Eddy covariance (EC) measurements have been made for many years (a number of medium term observation from 5-10 years). This technique yields values of fluxes observation of scalar atmospheric properties like momentum, heat, water vapor, carbon dioxide and methane fluxes by analyzing wind and scalar atmospheric data series.

FLUXNET[1] (Baldocchi et al, 2000) is a global network of micrometeorological tower sites that use eddy covariance methods to measure the exchanges of carbon dioxide, water vapor, and energy between the biosphere and atmosphere. It has brought together data sets of Eddy Covariance measurements from regional networks such as CarboEurope, AmeriFlux and LBA into one global network and currently 468 recording station are active with more than 200 stations with more than 10 years of data. Since this method gives a measurement of the total evapotranspiration it can be a reliable reference for validation of latent heat in models. However it should be noted that there is considerable debate in the community over the lack of energy closure from EC measurements [Charuchittipan et al, 2014; Foken, 2008; Stoy et al, 2013; Twine et al, 2000; and Wilson et al, 2002]

In ORCHIDEE surface vegetation heterogeneity is described using fractions of different Plant Functional types (PFTs), and energy, carbon and water fluxes are simulated based on these main vegetation types. Governing equations are the same for different PFTs, but they are distinguished by way of parametrization. Recent studies have detected some biases in soil evaporation, over some PFTs. Overestimation of bare soil evaporation in the 11 layer soil hydrological scheme in comparison to the previous 2 layer scheme (Servettaz, 2014), is assessed to be more important over forests with deciduous trees than other ecosystems. In these areas, simulated latent heat fluxes are more than observed amounts. Comparison is done mainly by data from FLUXNET micrometeorological tower sites.

Although it might not be likely at first, some evidence suggests that forest floor evaporation is often largely decoupled from net radiation (Baldocchi & Meyers, 1991), (Schaap & Bouten, 1997). Even during the dramatic changes associated with leaf emergence and senescence in a deciduous forest (Moore et al, 2000), and soil water content near the upper layer and leaf litter water content have been suggested as controls on forest floor evaporation (Wilson et al, 2000).

Over-evaporation during winter, could provoke diminished water reservoirs, thus limit evaporation in summer. Increased ratio of soil evaporation to the total evaporation (Interception, Transpiration and soil evaporation) can lead to under-estimation of other components of evaporation, thus causing unrealistic CO2 fluxes from vegetation and also affecting long-term plant evolution and

[1] Abbreviated form of FLUX NETwork. www.fluxnet.org

subsequent water stores. This shows the importance of simulating correctly the bare soil evaporation component of the evapotranspiration flux, for the energy balance but also for the carbon balance.

The objectives of this study are: (1) to evaluate the performance of ORCHIDEE in simulating bare soil evaporation in different soils and atmospheric conditions (2) test alternative approaches of BSE (bare soil evaporation) calculation in a simplified platform which only includes the BSE procedures of ORCHIDEE, regardless of other processes, (3) test alternative methods of BSE calculation in the full ORCHIDEE model platform using OD (Offline Decoupled) simulations at FLUXNET sites where both forcing and validation observations are available and eventually (4) asses if any of the alternative approaches for BSE calculation improve the simulation outputs of latent heat fluxes, especially in the areas where overestimation were detected.

2 Study background

Recently, emphasis has been placed on the importance of distinguishing between and quantifying the two major components of evapotranspiration (after accounting for evaporation of water intercepted by the canopy): evaporation from the soil and transpiration from plant (Cillegas et al, 2010).

Several solutions have been proposed solutions in order to account for bare soil evaporation more realistically [Milly, 1992; Sakaguchi & Zeng, 2009; de Rosnay & Polcher, 2002; Zhang et al, 2015]. All of these studies suggest or use methods of latent heat flux exchange between land and atmosphere which are drawn from either experimental or analytical solutions of relatively homogenous soils with little or no vegetation and include simplifications. These models share a basic structure which is shown in Figure 2-1. This figure shows a situation where the bare soil evaporation is mainly driven by the evaporation demand. Although same processes govern evaporation from soil in drier conditions (where water table is lower and the capillary fringe is not extended upto the soil surface), a relatively different behavior in evaporation patterns is observed (van de Griend & Owe, 1994).

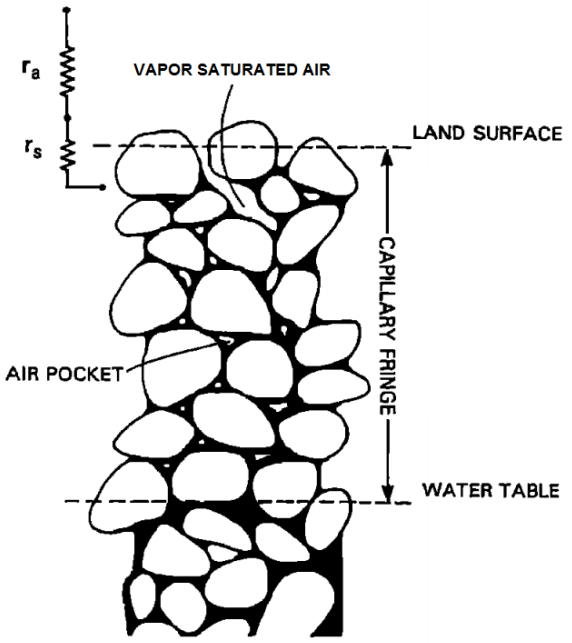

Figure 2-1. Schematic view of soil evaporation in bare soil

Soil evaporation is often introduced in models as one of the two following equations or a combination of them, which are here called Alpha (α) and Beta (β) methods.

$$E_{soil} = \rho_a \frac{\beta}{r_a}[q_s(T_s) - q_a] \qquad \text{Eq 2-1}$$

$$E_{soil} = \rho_a \frac{1}{r_a}[\alpha\, q_s(T_s) - q_a] \qquad \alpha, \beta = \text{effect of soil resistance} \qquad \text{Eq 2-2}$$

In these equations and also in Figure 2-1, $\rho_a$is the density of air $[kg.m^{-3}]$, $q_s(T_s)$ $[kg.kg^{-1}]$ is the specific humidity of saturated air at temperatures T_s (computed surface temperature $°K$), q_a is the specific humidity of the air at a standard level of measurement $[kg.kg^{-1}]$, r_a is the aerodynamic resistance of the boundary layer between the surface and the standard measurement level $[s.m^{-1}]$, and r_s is the soil resistance $[s.m^{-1}]$.

In this chapter methods of latent heat flux exchanges between soil and atmosphere are introduced, starting with the ORCHIDEE and following by other approaches in literature. Obviously, ORCHIDEE would be more discussed afterward and as a result, more details on procedures involved in ORCHIDEE are presented here.

The following section discusses the conceptual method of BSE computation in ORCHIDEE.

2.1 Heat flux presentation in ORCHIDEE

ORCHIDEE is a set of scripts mainly written in FORTRAN90 language. It has a modular structure and these modules work in a relatively independent manner. The total water flux from the land surface to the atmosphere in each grid cell is computed as the sum of snow sublimation, soil evaporation, transpiration by plants and evaporation of intercepted water by the canopy over all PFTs (Ringeval et al, 2012). Bare soil evaporation is handled in hydrol module. Since test simulations in ORCHIDEE's main platform are both time-taking and effortful, a simplified version of the BSE calculation subroutine is written in R language that facilitates further analysis. This script is meant to imitate what's being done in Hydrol module (originally *hydrol.f90* Fortran script). This module consists of three main reservoirs for canopy interception, snow pack and soil, for each of the grid-cells at each of time steps. BSE is computed in the soil reservoir and here we would mostly discuss this compartment of the module.

In ORCHIDEE the water redistribution scheme is described in (de Rosnay & Polcher, 2002) which is based on a transformed Richard equation:

$$\frac{\partial \theta}{\partial t} = \frac{\partial}{\partial z}\left(D(\theta)\frac{\partial \theta(z,t)}{\partial z} - K(\theta) \right) - s(z,t) \qquad \textit{Eq 2-3}$$

$$D\big(\theta(z,t)\big) = K(\theta(z,t))\frac{\partial \psi}{\partial \theta}(\theta(z,t)) \qquad \textit{Eq 2-4}$$

In which θ is the volumetric water content $(m^3.m^{-3})$, z (m) is the vertical coordinate, D $(m^2.s^{-1})$ is the soil water diffusivity, K $(m.s^{-1})$ is the unsaturated hydraulic conductivity, ψ (m) is the matric potential and t $(seconds)$ is time. In this equation, s $(m^3.m^{-3}.s^{-1})$ is the sink term representing plant root water extraction. The hydraulic parameters required by the diffusion equation solved in ORCHIDEE, are given in by (Van Genuchten, 1980) as a function of θ:

$$K(\theta) = K_s\sqrt{\theta_f}\left(1 - \left(1 - \theta_f^{\frac{1}{m}}\right)^m\right)^2 \qquad \textit{Eq 2-5}$$

$$D(\theta) = \frac{(1-m)K(\theta)}{\alpha m n}\frac{1}{\theta-\theta_r}\theta_f^{-1/m}.\left(\theta_f^{-\frac{1}{m}}-1\right)^{-m} \quad \text{Eq 2-6}$$

$$\psi(\theta) = \frac{-1}{\alpha}\left(\theta_f^{-1/m}-1\right)^{\frac{1}{n}} \quad \text{Eq 2-7}$$

$$\text{and } \theta_f = \frac{\theta-\theta_r}{\theta_s-\theta_r} \quad \text{Eq 2-8}$$

In these equations, α (m^{-1}) is inverse of air entry suction, m is a dimensionless parameter deduced from n, another dimensionless parameter, which are calculated from (d' Orgeval, 2006).

The top boundary condition of this model is substantial for soil-air interactions. This boundary depends on both the soil water content and atmospheric forcing. In ORCHIDEE, soil evaporation (result of the interaction between soil and atmosphere) depends on soil moisture and potential evaporation rate, which is calculate according to the Budyko formulation with some reductions.

In ORCHIDEE soil evaporation is calculated following a supply/demand approach as in these equations:

$$E_{soil} = \min\left(E_{pot}^{*}, Q_{up}\right) = \eta\, E_{pot} \quad \text{Eq 2-9}$$

$$E_{pot} = \rho_a \frac{q_s(T_s)-q_{air}}{r_a} \quad \text{Eq 2-10}$$

$$E_{pot}^{*} = \rho_a \frac{q_s(T_w)-q_{air}}{r_a} \quad \text{Eq 2-11}$$

This means at each time step, soil evaporation equals the minimum of the upward supply of water Q_{up} $(m.s^{-1})$ (which is derived from solving hydraulic equation of water movement) and $E_{pot}^{*}(m.s^{-1})$ (which is a modified potential evaporation from (Milly, 1992)), and unlike E_{pot} takes into account the specific humidity of saturated air at temperature T_w $(°K)$ instead of specific humidity at surface temperature T_s $(°K)$. T_w is the temperature of air in the evaporating surface which is hypothetically wet and is cooled down by evaporation process. In ORCHIDEE after redistribution of water content in previous time step, water diffusion is solved by dummy integration considering $E_{soil} = E_{pot}^{*}$, where E_{soil} $(m.s^{-1})$ is the actual soil evaporation. In this case if the soil water content doesn't go below residual content in none of the layers, then potential evaporation is sustained. Otherwise, this step is repeated assuming the water content of the first layer to be equal to residual water content, $\theta_r(m^3.m^{-3})$.

In which, ρ_a is the density of air, $q_s(T_s)$ $[kg.kg^{-1}]$ and $q_s(T_w)[kg.kg^{-1}]$ are the specific humidity of saturated air at temperatures T_s (computed surface temperature $°K$) and T_w(temperature of the hypothetically wet evaporating surface $°K$), q_{air} is the specific humidity of the air at a standard level of measurement and r_a is the aerodynamic resistance $[s.m^{-1}]$ of the boundary layer between the surface and the standard measurement level. However, in ORCHIDEE T_w is not computed separately and instead a correction factor, suggested by (Milly, 1992) is replaced so that:

$$E^{*}_{pot} = E_{pot} \cdot Corrfac \qquad \text{Eq 2-12}$$

The $Corrfac$ is a function of the empirically determined moisture availability function, and the maximum relative difference of E^{*}_{pot} and E_{pot}. It is also interpreted as a ratio of cooling rates via evaporation to radiation and sensible heat, and is calculated analytically for different aerodynamic resistances.

It is noteworthy to remind that potential evaporation is often calculated by means of meteorological data observed under non-potential conditions. Clearly, this is not the same rate as that which would be calculated (or observed) if the surface had been adequately supplied with water. Indeed, the partition of the available energy at the surface is related to the availability of water for evaporation, and this partition affects the temperature, air humidity and several other important state variables of the atmosphere. (Brustaert, 1982)

From the above formulation we define the multiplier η the stress factor as:

$$\eta = \frac{E_{soil}}{E_{pot}} \qquad \text{Eq 2-13}$$

η is calculated by a maximum of 4 steps. Within the procedure of calculation in ORCHIDEE, first E_{pot} is calculated from energy budget of the current one. Then a flux condition is tested by taking $E_{soil} = E^{*}_{pot}$. If then by dummy integration of the Richards equation, there were no node with water contents below residual content, all the demand is met (case 1). If in some nodes $\theta_i < \theta_r$, then the top layer water content is set to residual water content (Dirichlet condition-case 2). In any of the cases if the total soil moisture of the first (top) 4 layers, which represent the litter layer, are below the wilting point moisture, the stress factor is arbitrarily reduced by a factor 2 (case 3 and 4). The resulting stress factor will control E_{soil} and the surface energy budget of the next time step.

Given η of the previous time step and the energy budget of the current time step, E_{soil} is finally calculated. Then this evaporation amount is used to solve the water budget and updating θ_i of each node i over the soil profile. Consequently, this water content profile is used in the next time step to calculate η for that time step.

2.2 Different methods of soil evaporation calculation in models

Modelling efforts available in literature are categorized in 3 different major groups that I reviewed here (CLM, JULES and SiSPAT) followed by a number of other examples.

2.2.1 CLM (Community Land Model)

CLM modellers usually tried to reduce the fraction of bare soil evaporation from total evaporation, when it was unreasonably high. This was done by changing the linear relation between transpiration from plants and LAI to a nonlinear one. For instance Lawrence et al (2007) used a nonlinear relation in the Community Land Model (CLM), where the contribution of transpiration to total evapotranspiration rises sharply at low LAIs, hitting 50% at LAI=1, before reaching around 90% at LAI=5.

Oleson et al (2008) added a soil resistance term to their model, apart from aerodynamic resistance, to account for resistance to water vapor transport by molecular diffusion from the water surface in

the soil pores to the soil surface. This resistance term, r_{soil}, was based on work of Selleres et al (1992).

$$E_{soil} = \rho_a \, \beta[q_s(T_s) - q_a] \quad \text{Eq 2-14}$$

$$\beta = \frac{1}{r_a + r_{soil}} \quad \text{Eq 2-15}$$

$$r_{soil} = (1 - f_{sno}) \, e^{(8.206 - 4.255 s_1)} \quad \text{Eq 2-16}$$

Where f_{sno} is the fractional soil covered by snow and s_1 is the relative soil moisture of the first (top) layer with respect to saturation.

$$s_1 = \frac{\theta_{ice,1} + \theta_{liq,1}}{\theta_{sat,1}} \leq 1 \quad \text{Eq 2-17}$$

And $\theta_{ice,1}$, $\theta_{liq,1}$ and $\theta_{sat,1}$ are the volumetric ice, liquid water and saturation soil moistures in top layer.

Based on the work of Oleson et al (2008), in another study, (Sakaguchi & Zeng, 2009) changed in another study, the formulation for calculating soil evaporation and proposed new soil resistance and a new litter layer resistance. Their final formulation implements three resistances for aerodynamic, soil and litter resistances.

$$\beta = \frac{1}{r_a + r_{soil,new}} \quad \text{Eq 2-18}$$

$$r_{soil,new} = \frac{L}{D} \quad \text{Eq 2-19}$$

$$D = D_0 \theta_{sat}^2 \left(1 - \frac{\theta_r}{\theta_{sat}}\right)^{2+3b}, \quad \text{Eq 2-20}$$

$$L = d_1 \frac{\exp\left[(1 - \frac{\theta_1}{\theta_{sat}})^w\right] - 1}{e - 1} \quad \text{Eq 2-21}$$

Where D_0 $[m^2.s^{-1}]$ is the molecular diffusion coefficient of water vapor in the air, θ_{sat} is the volumetric water content at saturation, b is the fitting parameter for the soil water characteristic curve [Clapp & Hornberger, 1978; Cosby et al, 1984; Oleson, 2004], θ_r is the residual water content, d_1 $[m]$ is the thickness of the topsoil layer, e is a constant (2.718) and w is a parameter that controls concavity of the curve and is set to 5 in order to have an exponential shape found in experimental studies. Finally θ_1 is the volumetric content of the topsoil layer.

They also used a resistance term for the litter layer,

$$\beta = \frac{1}{r_a + r_{soil,new} + r_{litter}} \quad \text{Eq 2-22}$$

$$r_{Litter} = \frac{1}{0.004.\, u_*}\left(1 - e^{-L_{litter}^{eff}}\right), \quad \text{Eq 2-23}$$

Where u_* $[m.s^{-1}]$ is the friction velocity and L_{litter}^{eff} is defined by

$$L_{litter}^{eff} = L_{litter}[1 - \min(f_{litter}^{snow}, 1)] \quad \text{Eq 2-24}$$

$$f_{litter}^{snow} = \frac{d_{snow}}{0.05} \quad \text{Eq 2-25}$$

And in this study L_{litter} was simply taken as 1.

It is noteworthy to say that the presence of a litter layer on the ground controls soil evaporation via two basic mechanisms: through the attenuation of radiation flux into and from the ground (Baldocchi et al, 2000) and by increasing the resistance to water flux from the ground (Sakaguchi & Zeng, 2009)

2.2.2 SiSPAT (Simple Soil Plant Atmosphere Transfer Model)

In SiSPAT model [Braud et al, 1995; Braud, 2000], bare soil evaporation follows the atmospheric demand and the matric potential of the topsoil layer ($\psi(\theta_1)$ $[m]$) and is calculated using an aerodynamic resistance, r_a, from the following equation:

$$E_{soil} = \rho_a \beta[q_s^*(T_s) - q_{av}] \quad \text{Eq 2-26}$$

$$\beta = \frac{1}{r_a} \quad \text{Eq 2-27}$$

$$r_a = \frac{U_{av}}{\sigma(u_*)^2} \quad \text{Eq 2-28}$$

In this equation q_{av} is the specific humidity in the vegetation artificial level, which is different from the reference level (standard level of measurement). σ is the coefficient for the partition of momentum between bare soil and vegetation, u_* is the friction velocity and U_{av} $[m.s^{-1}]$ is the wind speed at vegetation level. e_{sat} $[Pa]$ is the saturated vapor pressure at the surface temperature, which is related to the soil surface temperature T_s, p_s $[Pa]$ surface atmospheric pressure, and the relative humidity at the surface h_u. The relative humidity at the surface is derived from Kelvin's law and depends on the matric potential and temperature (T_1 $[°K]$) of the top soil layer. This temperature could be taken almost equal to the temperature of the wet evaporating surface T_w , since almost all the evaporation from bare soil is from the upper most soil layer. The use of Kelvin's law partly realizes the coupling between the soil compartment and the interface and could be considered as a supply/demand approach.

$$q_s^* = \frac{0.622\, e_{sat}(T_s) h_u}{p_s - 0.378\, e_{sat}(T_s) h_u} \quad \text{Eq 2-29}$$

$$h_u = \exp\left(\frac{g.\psi(\theta_1)}{R.T_1}\right), \quad T_1 \approx T_w \quad \text{Eq 2-30}$$

It is noteworthy to remind that q_s (specific humidity) and $e_{sat}(T_s)$ (saturated vapor pressure) could be calculated from Eq 2-31and Eq 2-32:

$$q_s = \frac{0.622\ e_{sat}(T_s)}{p_s - 0.378\ e_{sat}(T_s)} \qquad \text{Eq 2-31}$$

$$e_s(T_s) = 6.112 \exp\left(\frac{17.67\ T_s}{T + 243.5}\right) \qquad \text{Eq 2-32}$$

Having in mind that $e_{sat}(T)$ is less than 9 kPa in environment temperatures below 45 °C and compared to p_s which is near 1 *atm*, the h_u factor in the dominator of q_s^* is of second order importance and effect in Eq 2-42.

In SiSPAT they propose using a two condition formula to relate water content to soil water pressure. To ensure that the volumetric water content is zero at a finite soil water pressure h_0 they use a modified Van Genuchten model into the dry domain. A threshold pressure h_c is prescribed such that A "Classical" Van Genuchten model is used for pressure higher than h_c and the modified model is used for pressure lower than h_c. This formula is only available when n the shape parameter in the Van Genuchten retention model is equal to $\frac{2}{1-m}$ (m is also a Van Genuchten parameter) and the residual water content is zero, and the procedure is iterative but converges rapidly. 1 and 2 indices for Van Genuchten parameters are for wet and dry domains respectively. Parameters of the formulation like h_{g2} and $n2$ must be determined such that the function and its first derivative are continuous for $h = h_c$.

$$\frac{\theta}{\theta_s} = \left[1 + \left(\frac{h}{h_{g1}}\right)^{n1}\right]^{-1+\frac{2}{n2}} \qquad h \geq h_c \qquad \text{Eq 2-33}$$

$$\frac{\theta}{\theta_s} = \left[1 + \left(\frac{h}{h_{g2}}\right)^{n2}\right]^{-1+\frac{2}{n2}} - \left[1 + \left(\frac{h_0}{h_{g2}}\right)^{n2}\right]^{-1+\frac{2}{n2}} \qquad h \leq h_c \qquad \text{Eq 2-34}$$

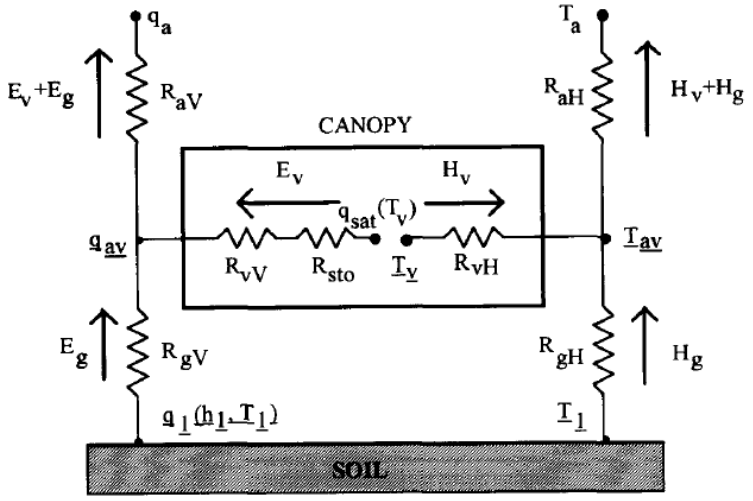

Figure 2-2 Schematic structure of SiSPAT's bare soil and vegetation sensible and latent heat flux exchange (Braud, et al., 1995))

2.2.3 JULES (Joint UK Land Environment Simulator)

Blyth et al (2010) reached some interesting results by comparing JULES (Joint U.K. Land Environment Simulator) results with FLUXNET observations. They observed that their model poorly represents evaporation if a fixed LAI is assumed where the vegetation has a strong seasonal phenology (e.g. crops and deciduous trees).

In their model the bare soil evaporation resistance is determined by the soil moisture concentration in the top soil layer (Best, et al., 2011):

$$E_{soil} = \rho_a \, \beta[q_s(T_s) - q_a] \qquad \textit{Eq 2-35}$$

$$\beta = \frac{1}{r_a + r_s} \qquad \textit{Eq 2-36}$$

$$r_s = 100 \, (\frac{\theta_c}{\theta_1})^2 \qquad \textit{Eq 2-37}$$

In the above equations, r_a the aerodynamic resistance is calculated using standard Monin-Obukhov similarity theory (Monin & Obukhov, 1954) and θ_c and θ_1 are the soil moisture concentrations in the critical point and first layer respectively. θ_c is defined by a matrix water potential of -33 kPa, which is stronger than matrix water potential in field capacity (-10 to -30 kPa). The use of the critical point enables vegetation to maintain an un-water stressed transpiration at values below field capacity (Best et al, 2011).

This parametrization was developed following problems identified with a previous scheme in JULES. The previous version of the scheme (MOSES) could not reproduce many features found in observational studies including, all three forecast components of evaporation being higher than observed, too low surface temperatures and lack of moisture stress on evaporation (Taylor & Clark, 2001).

2.2.4 Other models

Tang and Riley (2013) obtained a formulation which is applied only to the TopSoil Control Volume (TSCV) in which the soil evaporation resistance comprises two parts: (i) the resistance for the water vapor to diffuse through air-soil interface $r_a$and (ii) the resistance of soil which is itself a function of both the liquid flow resistance r_l and the vapor flow resistance r_v.

$$E_{soil} = \rho_a \, \beta[h_u q_s(T_s) - q_a] \qquad \textit{Eq 2-38}$$

$$\beta = \frac{1}{r_a + r_s} \qquad \textit{Eq 2-39}$$

$$r_s^{-1} = r_l^{-1} + r_v^{-1} = \frac{2\mu\theta_1 D_w}{\Delta z_1} + \frac{2\varepsilon D_g}{\Delta z_1} \qquad \textit{Eq 2-40}$$

$$D_w = K\frac{\partial\psi}{\partial\theta}, \quad \mu = \frac{\rho_l}{\rho_a q_a} \qquad \textit{Eq 2-41}$$

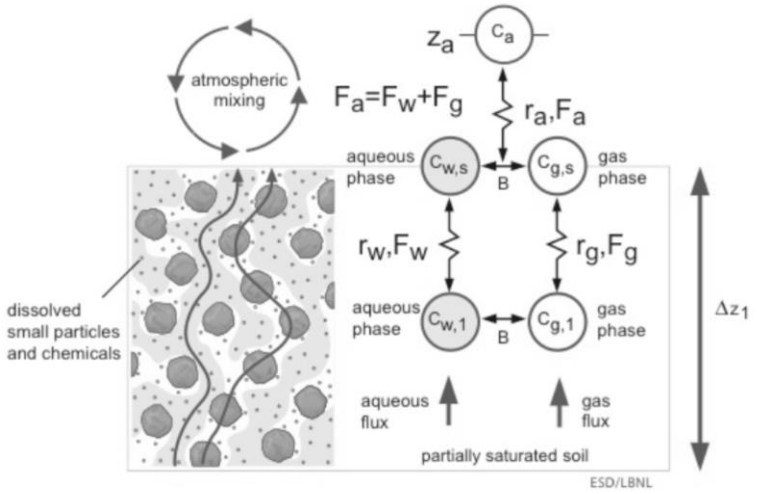

Figure 2-3 Schematic of the topsoil control volume interface and atmospheric or canopy air concentration (Tang & Riley, 2013)

In these equations K is the hydraulic conductivity $[m.s^{-1}]$, ψ is the soil matric potential $[m]$, ε is the air filled porosity $[m^3.m^{-3}]$, D_g is the water vapor diffusivity in soil $[m^2.s^{-1}]$, ρ_l and ρ_a are the liquid water and air density, $q_s(T_s)$ is the specific humidity in the topsoil and Δz_1 is the thickness of the TSCV.

In another recent study Zhang et al, (2015) developed an analytical model for predicting the surface resistance to vapor transport through the soil-air interface during the soil drying process. In this study they propose an analytical model to describe surface resistance for different water contents. When the vaporization plane[2] is in the topmost soil layer, TSL, (pond like accumulated water), there is no or very small resistance. When the vaporization plane develops below the TSL, the model predicts surface resistance by taking into account the development of the dry soil layer, which is a major barrier for the transport of water vapor. The authors believe that by consideration of the soil pore size distribution, the model is applicable to different soil types. The analytical solution is a long formulation and would not be brought here. This model treats surface resistance in two different ways. First when the vaporization plane remains in the TSL, where the model describes the surface resistance by vapor transport through EDL (External diffusive layer) and hydraulic connection between the capillary water. When this vaporization plane develops below TSL, the model estimates the thickness of the dry soil layer in NSL (Near Surface Layer). This procedure is regulated by using a parameter K_{vr}, the relative vapor conductance and a linear relationship regulates the contribution of each conductance to resistance:

$$\mathrm{r_s} = \frac{1}{\mathrm{K_v}} = \frac{\delta}{\mathrm{D_0 K_{vr}}} \qquad \textit{Eq 2-42}$$

In this equation D_0 is the vapor diffusivity in the air, δ is the thickness of the EDL (External Diffusive Layer) and K_v is the vapor conductance. K_{vr} is the relative vapor conductance which

[2] The plane where the liquid water is intensively converted into the vapor phase

equals unity when the soil surface is fully covered by liquid and decreases with the desaturation of the vaporization plane and thickening of the dry soil layer.

Brutsaert (2014) introduced an analytical solution for soil evaporation, with simplification for rather long periods of time. He compared the results of the proposed formulation to extensive experimental observation from [Jackson et al, 1973; Jackson, 1973] and excellent agreement of different features of the solution of the linearized Richards equation was reached. This solution is solely valid for the second stage of evaporation where the evaporation from bare soil is mostly limited by soil water availability and not by atmospheric demand. Figure 2-4 shows the evolution of daily evaporation in a case study. The formulation of the analytical solution is brought below.

$$E = (\theta_i - \theta_0)(\overline{D}/\pi)^{0.5} t^{-0.5} \qquad \text{Eq 2-43}$$

There, θ_i is the initial (uniform) water content at the start of the second stage of evaporation, θ_0 is the air-dry water content near the surface, $\overline{D}$ is a constant weighted soil water diffusivity and t is time. It should be noted that as the author mentions, for soil controlled evaporation process at time scale of a day or longer, useful results can be obtained by making a number of simplifications. However such simplifications might not be valid for shorter time scales (Brutsaert, 2014). This study is a bit more discussed in the Appendix.

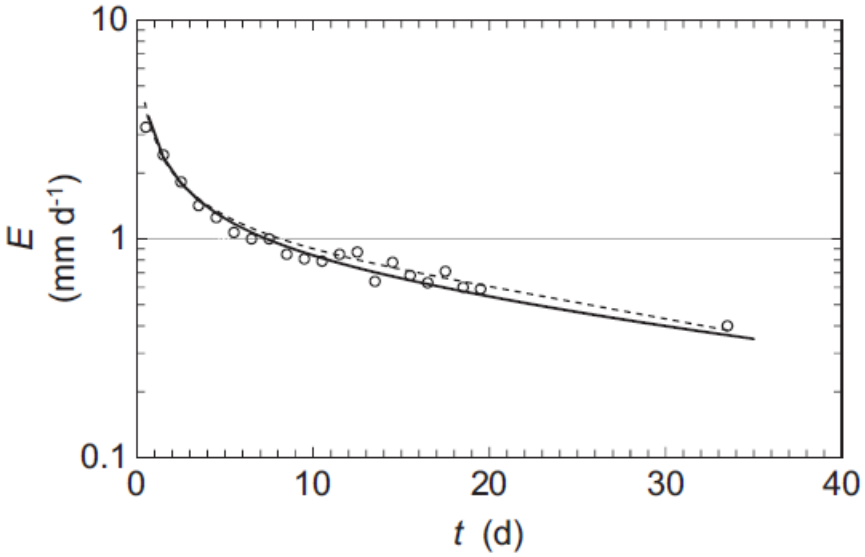

Figure 2-4 Evolution of daily evaporation (in mm d $^{-1}$) from a bare Adelanto loam soil, with time t (in days) after start of soil-controlled evaporation as measured in the study of Jackson [1973]

2.3 Synthesis

Soil evaporation calculation formulation can be categorized with regard to different factors. They could be categorized based on their supply/demand approach or those that only consider demand. They could also be categorized into so called α and β methods, in which the reduction factor is either applied to the whole potential evaporation term or to the specific humidity term in it or both. To summarize what has been discussed in previous chapters, a summary of soil evaporation calculation approaches are brought in Table 2-1.

Table 2-1 Representation of Soil evaporation and resistances in literature

Type of formulation	Study	formulation	Description
$E_{soil} = \rho_a \beta [q_s(T_s) - q_a]$	ORCHIDEE	$\beta = Corrfac.\frac{1}{r_a}$	Based on the work by (de Rosnay & Polcher, 2002) Actually the soil evaporation is of the form of a min function of supply and demand: $\mathrm{E_{soil}} = \min(\mathrm{E^*_{pot}}, \mathrm{Q_{up}})$
	Oleson et al., 2008	$\beta = \frac{1}{r_{soil} + r_a}$ $r_{soil} = (1 - f_{\mathrm{sno}})\, e^{(8.206 - 4.255 s_1)}$	Based on the work by Sellers et al., 1992.
	Best. et al., 2010	$\beta = \frac{1}{r_{soil} + r_a}$ $r_{soil} = 100\,(\frac{\theta_c}{\theta_1})^2$	θ_c is defined by a matrix water potential of -33 kPa
	Zhang et al., 2015	$\beta = \frac{1}{r_{soil} + r_a}$ $r_{soil} = \frac{1}{K_v} = \frac{\delta}{D_0 K_{vr}}$	
$E_{soil} = \rho_a \beta\, [\boldsymbol{\alpha}\, q_s(T_s) - q_a]$ $\alpha = h_u = exp\left(\frac{g.\psi(\theta_1)}{R.T_1}\right)$	Sakaguchi and Zeng 2009	$\beta = \frac{1}{r_{soil} + r_a + r_{litter}}$ $r_{soil} = \frac{d_1.\left\{exp\left[\left(1 - \frac{\theta_1}{\theta_{sat}}\right)^w\right] - 1\right\}}{\left[D_0 \theta_{sat}^2 \left(1 - \frac{\theta_r}{\theta_{sat}}\right)^{2+3b}\right](e-1)}$ $r_{litter} = \frac{1}{0.004.u_*}\left(1 - e^{-L^{eff}_{litter}}\right)$	w, e And b are constants. d_1 Is the thickness of the topsoil layer.
	SiSPAT	$\beta = \frac{1}{r_a}$ $r_a = \frac{U_{av}}{\sigma(u_*)^2}$	The evaporation is only dependent on atmospheric demand and α.
	Tang and Riley, 2013	$\beta = \frac{1}{r_{soil} + r_a}$ $r_{soil} = \frac{\Delta z_1}{2\alpha\theta_1 D_w + 2\varepsilon D_g}$	The method is based on differentiating between vapor flow resistance and liquid flow resistance (Tang & Riley, 2013)

3 Preliminary tests with a simplified model

In this chapter we aims to diagnose current behavior of bare soil evaporation (which would be briefly called BSE from now on) in a simplified version of ORCHIDEE written in R scripts, considering several hypothetical initial conditions and environmental characteristics (soil moisture profile, soil class, atmospheric demands,..). Alternative bare soil evaporation formulations in technical literature are then replaced in the simplified ORCHIDEE platform to find out if there is any substantial discrepancy in the soil evaporation response to atmospheric demands in ORCHIDEE in comparison to other methods.

3.1 Simulation in R

3.1.1 Principals of calculation code

As discussed before, the core of *hydrol.f90* is simulated in the R software platform, considering a wide range of atmospheric demands and soil characteristics. This is a simplification of *hydrol* module since only the dummy integration of the Richard's equation Eq 2-3 is done. In the actual *hydrol.f90* in FORTRAN, in addition to dummy integration some smoothing processes are included, which do not exist in the R code.

This simplified modeling is only for one time period and one grid cell. Meaning that there are no inter-cell interactions and fluxes. Only vertical fluxes are taken into account and the soil is considered to be bare, without any vegetation and transpiration due to plants. Similarly, as in ORCHIDEE, the soil column is about 2 meters deep. The bottom boundary condition is taken to be a free drainage condition by using a parameter (Fc) which could be modified and the default value is 1 in ORCHIDEE. Minimum and maximum water contents (corresponding to residual and saturation water contents) are kept contant for different soil classes to make comparison easier with time evolution.

In *hydrol.f90*, as mentioned before, after testing the extraction of potential evaporation from soil, if the volumetric water content in any of the calculation nodes is lower than the residual water content, then a limiting condition (Dirichlet condition) is set, which puts the first layer's volumetric water content equal to residual water content and severely controls evaporation from soil. This also exists in the R code and we will discuss it in the Results section (Section 5.1).

To have a wide variety of environmental initial conditions and atmospheric conditions, a combination of different cases are investigated. Parameters forming these cases are discussed in the following sub-sections.

3.1.2 Forcing Conditions

- *Aerodynamic resistance*

The transfer of heat and water vapor from the evaporating surface into the air above the canopy is determined by the aerodynamic resistance. This resistance is mostly dependent on roughness length of the surface and wind speed. In this study 12 levels of aerodynamic resistances were considered from 10 $[s.m^{-1}]$ to 120 $[s.m^{-1}]$ based on (Katerji, 1977) [see appendix].

- *Surface temperature*

Land surface temperature T_s ($°K$) is used to calculate saturated surface specific humidity $q_s(T_s)$ $[kg.kg^{-1}]$ in soil evaporation formulation. Very little evaporation happening below freezing temperature, the lower boundary of the temperature levels is 273 $°K$ (0 $°C$). Similarly, no water being available to evaporate in areas with surface temperature over 30 $°C$, the upper boundary is 303 $°K$. Consequently, 7 surface temperature levels 5 $°K$ apart were chosen between 273 and 303 $°K$.

- *Air specific humidity*

Air specific humidity q_{air} $[kg.kg^{-1}]$ is the ratio of water vapor mass to the air parcel's total. In this study 10 levels of specific humidity of air is used between 0.003 to 0.03 $[kg.kg^{-1}]$.

- *Soil moisture profile*

Different shapes of soil moisture profile are considered here. These 18 shapes include both extreme dry and wet conditions. All of them range between minimum and maximum soil moisture contents (residual and saturation soil moisture). Figure 3-1 shows these different shapes.

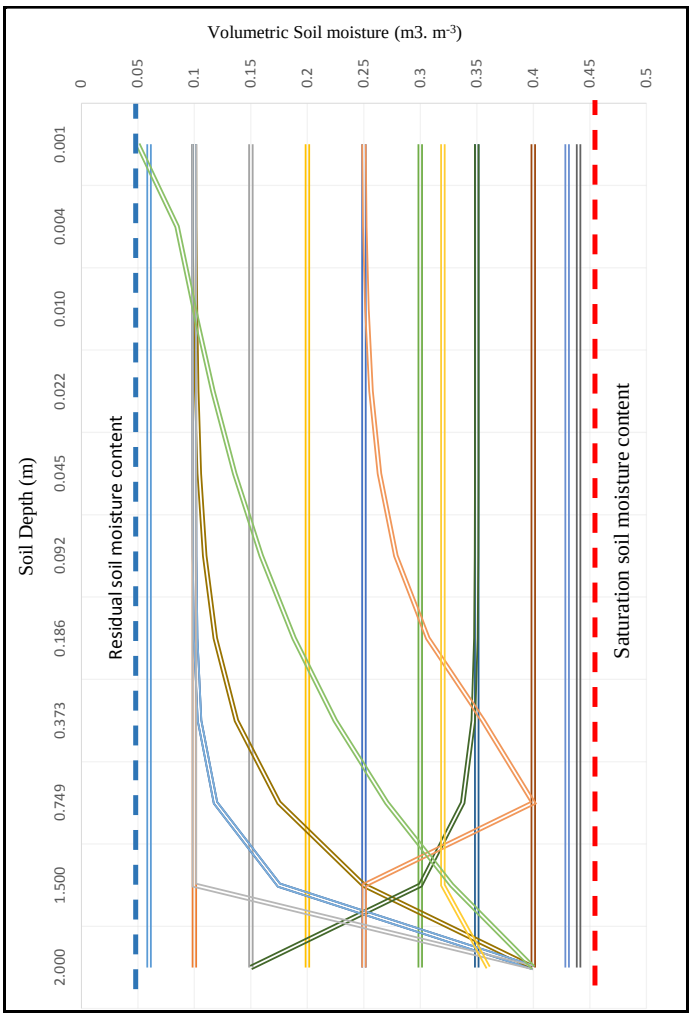

Figure 3-1 Different hypothetical Soil moisture profiles considered in the study

- *Soil classes*

Like in ORCHIDEE we classified 12 type of soils (based on their composing elements) each of which is different from the other in its saturated hydraulic conductivity (K). Table 3-1 shows the saturated conductivity of these soil classes. Different saturated hydraulic conductivity leads to different van Genuchten parameters ($\alpha, m \; and \; n$, Eq 2-5, Eq 2-6 and Eq 2-7, controlling the diffusivity and fluxes.

Table 3-1 Different soil classes and their corresponding saturated conductivity in the study

Soil Class	Saturated Conductivity K ($m.s^{-1}$)
Clay	1.7E-07
Clay Loam	6.4E-07
Loam	3.7E-06
Loamy Sand	1.7E-05
Silt	6.9E-07
Silty Loam	1.9E-06
Silty Clay	2.5E-07
Silty Clay Loam	4.2E-07
Sand	5.8E-05
Sandy Cly	3.3E-07
Sandy Clay Loam	1.2E-06
Sandy Loam	1.0E-05

These sets of soil and atmospheric conditions form more than 180,000 cases, for each of which the performance of different models (ORCHIDEE, SiSPAT, JULES, CLM,..) is evaluated. Since some combinations of these environmental variable may lead to physically unfeasible evaporative demands, the potential evaporation is bounded between 0-20 mm/day.

3.2 R simulation results

As it was mentioned in the previous chapter, the evaporative demand is calculated using a set of different surface temperatures, air specific humidity and aerodynamic resistances.

The first issue that one notices is that ORCHIDEE model performs with a double inclination, either toward meeting the evaporation demand or to go through the Dirichlet condition and allow very small evaporations. Figure 3-2 shows the density of the evaporation ratio (the ratio of actual evaporation to potential evaporation) in ORCHIDEE model. The densities are calculated for 0.01 band width. One can easily recognize that, at least within the range of the assumed soil moisture profiles, there is no evaporation event between 0.05 to 0.95 of the potential evaporation amount. While saturated soils, or soils with surface layer saturated water content, always meet the whole atmospheric demands, soils with lower water contents are often not allowed to generate evaporations as a fraction of the evaporation demand and are forced to meet the whole demand.

Imposing the corrected potential rate (E^*_{pot}) to the soil seems to be somewhat problematic. In some cases, although the soil may be wet (near saturation), the slow movement of water (liquid or vapor) inside soil pores, makes it impossible to meet the corrected potential demand of evaporation and the ORCHIDEE procedure would turn to the Dirichlet condition (with very low fluxes), hence preventing evaporations near but less than E^*_{pot}.

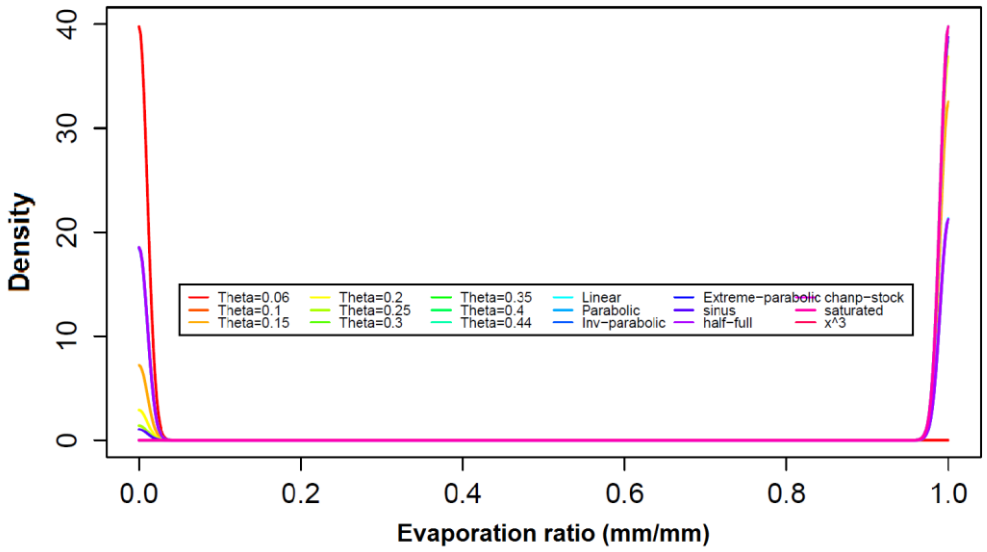

Figure 3-2 Density of the ratio of Actual evaporation to potential evaporation in ORCHIDEE

This is mainly because of the process of bare soil evaporation in ORCHIDEE, as discussed before, involves a Dirichlet case, which can either allow near potential evaporations from the soil or very low fluxes corresponding to soil with residual water content. This is in contrast with other approaches however, where usually a reduced fraction of potential evaporation (with regards to soil water contents) is demanded to the soil. In the following figures a comparison of the evaporation ratio (ratio of actual soil evaporation to potential evaporation) for regular and Dirichlet-case procedures. In these analyses, different approaches which were discussed in the literature were used to investigate difference behaviors [see Table 2-1]. All approaches have been thoroughly discussed in the bibliography section (section 2.2 page 7), however for SiSPAT parametrization a slight modification was done. In *SiSPAT-Modified* the h_u term in the dominator is omitted as in :

$$SiSPAT \qquad q_s = \frac{0.622\, e_{sat}(T_s) h_u}{p_s - 0.378\, e_{sat}(T_s) h_u} \qquad \text{Eq 3-1}$$

$$SiSPAT - Modified \qquad q_s = \frac{0.622\, e_{sat}(T_s) h_u}{p_s - 0.378\, e_{sat}(T_s)} \qquad \text{Eq 3-2}$$

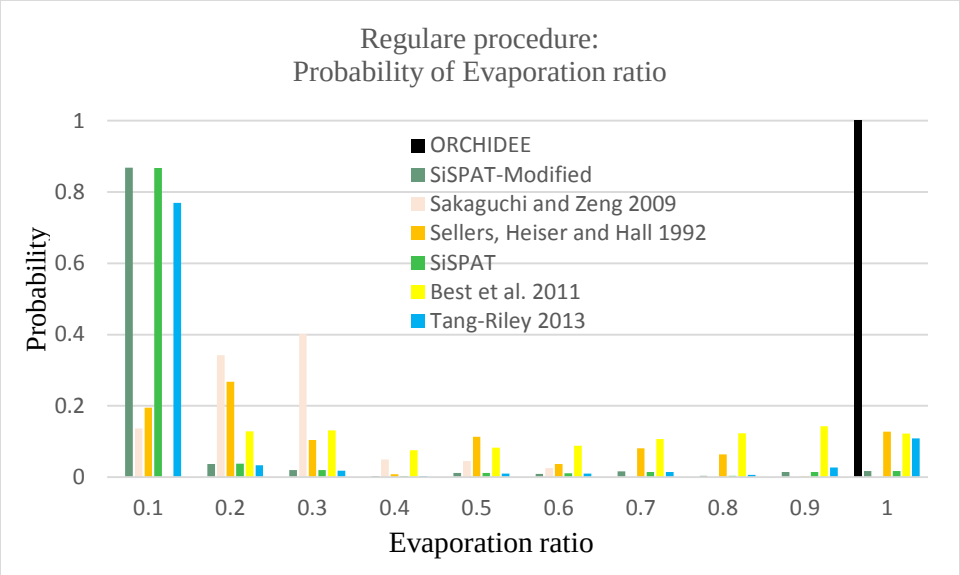

Figure 3-3 Probability of different evaporation ratios in regular procedure (non-dirichlet)

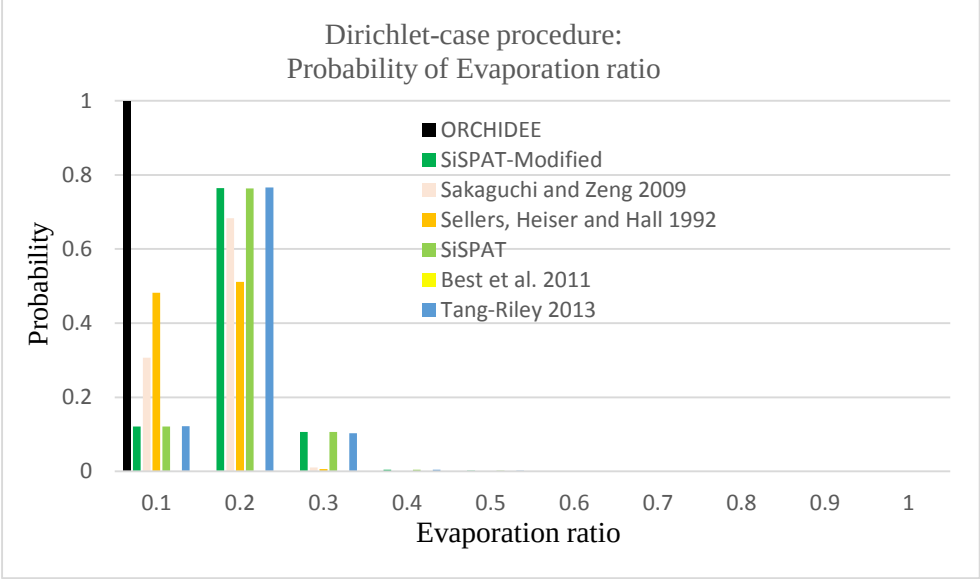

Figure 3-4 Probability of different evaporation ratios in Dirichlet procedure

As it could be noticed from the figures above, ORCHIDEE never results in evaporation ratios between 0.05-0.95 and is inclined to 0 and 1. In the regular procedure none of the approaches except ORCHIDEE led to high numbers of cases that meet the whole demand. It should be noted that in ORCHIDEE the potential evaporation is reduced by the flux condition test embedded in it, that doesn't exist in the R simplified version.

4 Test with ORCHIDEE at FLUXNET stations

At this stage, to validate simulations of different approaches to observed values of soil evaporation, we would tested alternative approaches in the platform of ORCHIDEE model and run a set of simulations in comparison to FLUXNET data.

4.1 Methods

After analysis of the behavior of different approaches involving ORCHIDEE in R software platform, a selection of approaches has been incorporated into ORCHIDEE platform. This stage requires great attention since debugging and calculation takes a lot of time and any small error in coding will lead to large discrepancies in the output.

4.1.1 ORCHIDEE

As it was described in ORCHIDEE explanation (section 2.1) water movement and energy fluxes related to it are all brought in hydrol module (*hydrol.f90*). In this module sub modules calculate different procedures involve (for example: *hydrol_waterbal* checks the water balance or *hydrol_flood* computes the evolution of the surface reservoir). The soil hydraulics and flux exchange compartment of ORCHIDEE (*hydrol_soil*) works with a set of forcing introduced to it:

- Meteorological forcings: precipitation, wind and turbulence;
- Photosynthesis forcings: radiation on land is dependent on LAI, which is in ORCHIDEE to a great extent prescribed depending on predefined PFT (Plant functioning types)and ignores known physiological constraints such as longevity and hydraulic conductance (Paylin et al, 2015).
- Soil properties: soil texture is read as USDA texture classes, provided at $^{1}/_{12}$ ° resolution (Reynolds et al, 2000).

4.1.2 FLUXNET datasets

Eddy covariance (EC) measurements can be a reliable reference observation for the performance evaluation of land surface models. These ground based observations of surface energy fluxes could be used to compare total latent and sensible heat fluxes, CO2 exchanges, soil temperature and some other surface variables. Since latent heat fluxes involve transpiration, interception and bare soil evaporation, an important question is to disentangle contribution of these components in total evapotranspiration. Some methods have been studied using isotopes, but they are still under debate.

Eddy covariance towers measure variables at 30 second time steps. By averaging the measurement and taking care of missing data, the final outputs are in 30 minutes time steps and contain several variables:

- Meteorological: Rainfall, wind speeds, surface pressure
- Fluxes: Latent heat flux, sensible heat flux, soil heat flux, Ecosystem respiration,..
- Radiation: Net radiation, incident longwave/shortwave radiation
- Temperatures: air temperature, soil temperature,..

4.1.3 Performed simulations in ORCHIDEE

Using libIGCM[3], one can run a set of simulations and then evaluate the performance of ORCHIDEE against in-situ data of FLUXNET eddy covariance sites where Carbon (NEE, GPP, TER) and energy fluxes (latent heat, sensible heat) and also meteorological measurements are available. In this study we used this library in order to run a couple of simulation with comparison to FLUXNET observations. These simulations are taken from literature (CLM: Best et al, 2011; Selleres et al. 1992; SiSPAT: Braud et al. 1995).

❖ *Selection of stations*

Since most of the BSE discrepancies were detected in areas with deciduous forest vegetation cover, two PFTs, deciduous broadleaf forests and low-height plants (e.g. crops, grasslands,..) are selected for vis-à-vis comparison of ORCHIDEE and alternative approaches. Ten FLUXNET stations located in grasslands, croplands and temperate deciduous forest are chosen for cross validation.

Table 4-1 shows specifications of these selected stations. The criteria for choosing these stations were their data availability (freely available) the length and continuity (few missing data), of the records and vegetation cover at the station. Figure 4-1 shows approximate location of these 10 sites.

[3] **Lib**rary for **I**PSL **G**lobal **C**limate **M**odeling Group

Table 4-1 The specification of the FLUXNET stations used in validation

Site Name	Fluxnet ID	Country	Coordinate		Year of data availability																									Description
			Latitude	Longitude	1991	1991	1991	1991	1991	1991	1991	1991	1991	2000	2001	2002	2003	2004	2005	2006	2007	2008	2009	2010	2011	2012	2013	2014	2015	
Bondville	US-Bo1	Illinois, USA	40.0062	-88.2904						■	■	■	■	■	■	■	■	■	■	■	■	■	■	■	■	■	■	■	■	Agriculture, Annual rotation between corn (C4) and soybeans (C3). The field was planted with corn (2005 & 2007), and soybeans (2006 & 2008)
Bugacpuszta	HU-Bug	Hungary	46.6911	19.6013												■	■	■	■	■	■	■								Bugacpuszta is currently Active, core measurements presently being made.
Collelongo- Selva Piana	IT-Col	Italy	41.8494	13.5881						■	■	■	■	■	■	■	■	■	■	■	■	■	■	■	■	■	■			Natural origin and managed, 84 km E from Rome; 56 km S from L'Aquila. Deciduous broadleaved forest.
Fort Peck	US-FPe	Montana, USA	48.3077	-105.1019									■	■	■	■	■	■	■	■	■	■	■	■	■	■	■	■	■	The Fort Peck, Montana station is located on the Fort Peck Tribes Reservation, approximately fifteen miles north of Poplar, Montana.
Harvard Forest EMS Tower (HFR1)	US-Ha1	Massachusetts, USA	42.5378	-72.1715	■	■	■	■	■	■	■	■	■	■	■	■	■	■	■	■	■	■	■	■	■	■	■	■	■	The Harvard Forest tower is on land owned by Harvard University.Climate measurements have been made at Harvard Forest since 1964.
Hesse Forest- Sarrebourg	FR-Hes	France	48.6742	7.0656						■	■	■	■	■	■	■	■	■	■	■	■	■	■	■	■	■	■	■	■	60 km East of Nancy, deciduous broadleaf forest, beech. Has experienced some thinning management. Natural origin and managed, mediterranean/montane climate.
Mead - irrigated continuous maize site	US-Ne1	Nebraska, USA	41.1651	-96.4766											■	■	■	■	■	■	■	■	■	■	■	■	■	■	■	This site is irrigated with a center pivot system. A tillage operation (disking) was done just prior to the 2001 planting to homogenize the top 0.1 m of soil.
Soroe- LilleBogeskov	DK-Sor	Denmark	55.4859	11.6446						■	■	■	■	■	■	■	■	■	■	■	■	■	■	■	■	■				Mediterranean/montane. Site is subject to dominant winds from the west, with air masses coming from the Atlantic Ocean driven by low pressure systems bringing temperature and humid air and precipitation.
Vaira Ranch	US-Var	California, USA	38.4067	-120.9507										■	■	■	■	■	■	■	■	■	■	■	■	■	■	■	■	The Vaira Ranch site is classified as a grassland dominated by C3 annual grasses. Species include a variety of grasses and herbs. Growing season is confined to the wet season only, typically from October to early May.
Willow Creek	US-WCr	Wisconsin, USA	45.8059	-90.0799								■	■	■	■	■	■	■	■	■	■	■	■							The surrounding stand occupies about 260 ha and is relatively homogeneous within 0.6 km of the tower. . The stands are conversions from the old-growth hemlock-hardwood forests to sugar maple-aspen-yellow birch forests.

Figure 4-1 Location of the selected FLUXNET sites on a map

❖ *Definition of simulations*

FLUXNET measurements are compared with reference simulations of original ORCHIDEE and seven different approaches for bare soil evaporation to rank performances of these approaches. Although the primary variable to compare is latent heat flux, some other variables are also investigated (like, GPP,…). One of these alternative approach to calculate bare soil evaporation is based on SiSPAT model (Braud et al, 1995). While the two resistance terms used are categorized as the so called β methods, this last approach is under the α methods. It should be mentioned here that these categories are not strict and a combination of the two has been used in literature (Sakaguchi & Zeng, 2009). At the end, an activation of rootsink subtraction from soil moisture within the ORCHIDEE code was also tested[4]. A combination of rootsink activation and three mentioned alternative approaches was also tested. To summarize these seven approaches they are brought in Table 4-2 below.

Table 4-2 specification of the three alternative bare soil evaporation formulations used in the study

Type		Formulation	Reference
Resistance terms		$E_{soil} = \rho_a \frac{\mathbf{1}}{\boldsymbol{r_a + r_s}} [q_s(T_s) - q_a]$ $r_s = e^{(8.206 - 4.255 s_1)}$	(Sellers, et al., 1992)
		$E_{soil} = \rho_a \frac{\mathbf{1}}{\boldsymbol{r_a + r_s}} [q_s(T_s) - q_a]$ $r_s = 100 \left(\frac{\theta_c}{\theta_1}\right)^2$	(Best, et al., 2011)
Using relative humidity		$E_{soil} = \rho_a \frac{\mathbf{1}}{\boldsymbol{r_a}} [h_u q_s(T_s) - q_a]$	Based on SiSPAT model (Braud, et al., 1995)
Rootsink activation +	Original ORCHIDEE	Original ORCHIDEE + rootsink activation in the second dummy integration	ORCHIDEE documentations
	Resistance terms	$E_{soil} = \rho_a \frac{\mathbf{1}}{\boldsymbol{r_a + r_s}} [q_s(T_s) - q_a]$ $r_s = e^{(8.206 - 4.255 s_1)}$	(Sellers, et al., 1992)
		$E_{soil} = \rho_a \frac{\mathbf{1}}{\boldsymbol{r_a + r_s}} [q_s(T_s) - q_a]$ $r_s = 100 \left(\frac{\theta_c}{\theta_1}\right)^2$	(Best, et al., 2011)
	Using relative humidity	$E_{soil} = \rho_a \frac{\mathbf{1}}{\boldsymbol{r_a}} [h_u q_s(T_s) - q_a]$	Based on SiSPAT model (Braud, et al., 1995)

[4] In the procedure of bare soil evaporation limiting factor calculation of ORCHIDEE (calculation of water stress factor), this part was missing.

4.2 Results

To summarize all results four of the alternative effort studied is presented here. These four alternative include 1. Adding SiSPAT-based relative humidity, 2. Using resistance terms by Sellers et al. (1992), 3. Resistance term by Best et al. (2011) and 4. Combination of rootsink activation and the soil resistance term of Sellers et al. (1992). These four are chosen because each of them represent a conceptual view of the limitations on BSE from the soil conditions. Other approaches' results were very close to these chosen ones. Table 4-3 and Table 4-4 makes a comparison between statistical indexes, assessing the performance of all 7 approaches investigated in this study.

Table 4-3 Average observed and simulated latent heat flux in 10 chosen FLUXNET sites

Fluxnet station code		Average Latent heat (W/m^2)								
		Fluxnet Observation	ORCHIDEE	Best et al. 2011	Rootsink activation	Rootsink + Best et al. 2011	Rootsink + Sellers et al 1992	Rootsink + SiSPAT	Sellers et al 1992	SiSPAT
Temperate deciduous broadleaf forest	DK-Sor	31.3	55.7	49.0	32.0	50.1	31.1	25.2	28.5	25.2
	FR-Hes	25.9	68.4	62.5	48.9	63.2	46.6	38.5	43.4	38.5
	IT-Col	24.7	61.2	56.7	42.1	58.1	42.6	34.2	39.7	34.1
	US-Wcr	27.6	47.8	103.6	37.6	103.6	34.8	103.6	32.6	103.6
	US-Ha1	32.6	63.8	118.8	48.7	118.8	46.9	118.8	44.1	118.8
Cropland C4	US-Ne1	49.7	44.6	44.3	46.7	44.6	40.6	37.9	40.1	37.8
	US-Bo1	46.7	47.7	46.9	43.1	46.8	42.1	34.2	40.1	34.2
Grassland C3	HU-Bug	35.9	37.2	37.0	30.3	37.4	36.2	30.1	33.3	29.9
	US-Fpe	23.8	23.8	23.8	26.3	23.9	23.8	23.6	23.7	23.6
	US-Var	22.9	34.4	34.2	23.4	34.6	34.0	30.8	32.4	30.7

Table 4-4 Root mean square error of simulated vs observed latent heat flux in 10 chosen FLUXNET sites

Fluxnet station code		Root mean square error (simulation vs Observed fluxnet latent heat)							
		ORCHIDEE	Best et al. 2011	Rootsink activation	Rootsink + Best et al. 2011	Rootsink + Sellers et al 1992	Rootsink + SiSPAT	Sellers et al 1992	SiSPAT
Temperate deciduous broadleaf forest	DK-Sor	33.7	24.9	16.5	25.8	18.8	20.7	17.9	20.7
	FR-Hes	62.6	42.6	31.9	43.4	32.9	28.2	29.0	28.2
	IT-Col	43.5	39.6	28.4	41.4	32.8	28.9	29.4	28.8
	US-Wcr	26.9	88.3	20.4	88.3	22.5	88.3	21.1	88.3
	US-Ha1	36.5	93.2	24.9	93.2	25.7	93.2	23.8	93.2
Cropland C4	US-Ne1	23.6	23.0	23.0	23.6	23.7	28.3	22.1	28.3
	US-Bo1	19.7	18.9	20.9	19.8	23.7	29.7	22.6	29.7
Grassland C3	HU-Bug	12.1	11.8	12.1	12.3	16.5	19.2	16.5	19.1
	US-Fpe	20.4	20.2	18.1	20.8	20.6	21.2	19.1	21.0
	US-Var	17.9	18.4	8.5	19.2	24.1	27.1	23.7	27.2

Figure 4-2, Figure 4-3, Figure 4-4, and Figure 4-5 show the performance of alternative approaches to model bare soil evaporation. Here, to be brief, just two FLUXNET station results are shown (station codes: FR-Hes and US-Var) one located in a broadleaf deciduous forest and the second in a grassland, to provide performance results for different PFTs. In these figures solid black line is FLUXNET in-situ measurements, red line indicates original ORCHIDEE approach and solid green line is the alternative approach.

FR-Hes

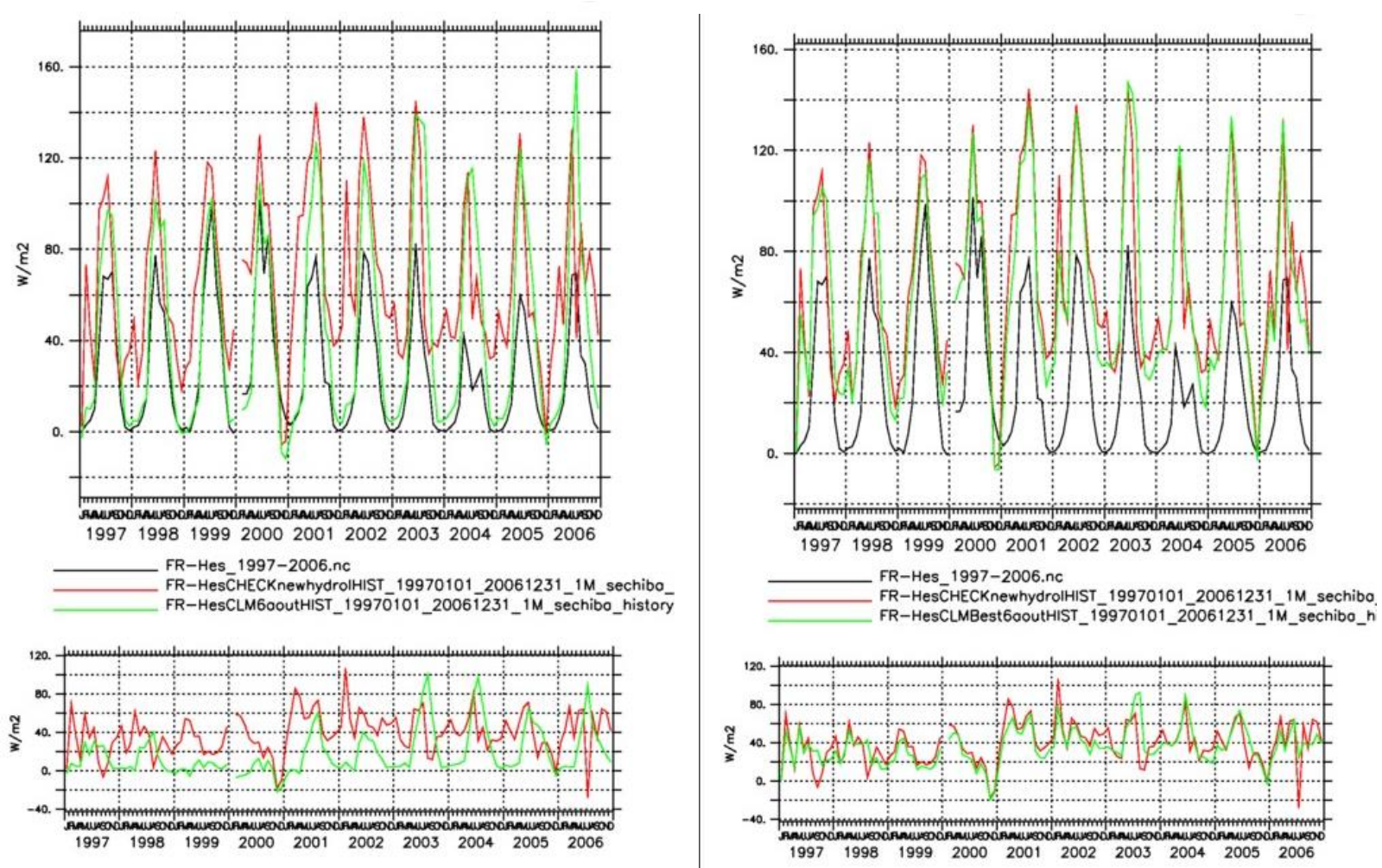

Figure 4-2 Cross validation results of Latent heat flux FR-Hes fluxnet station
left: Resistance term by (Sellers, et al., 1992) right: Resistance term by (Best, et al., 2011)

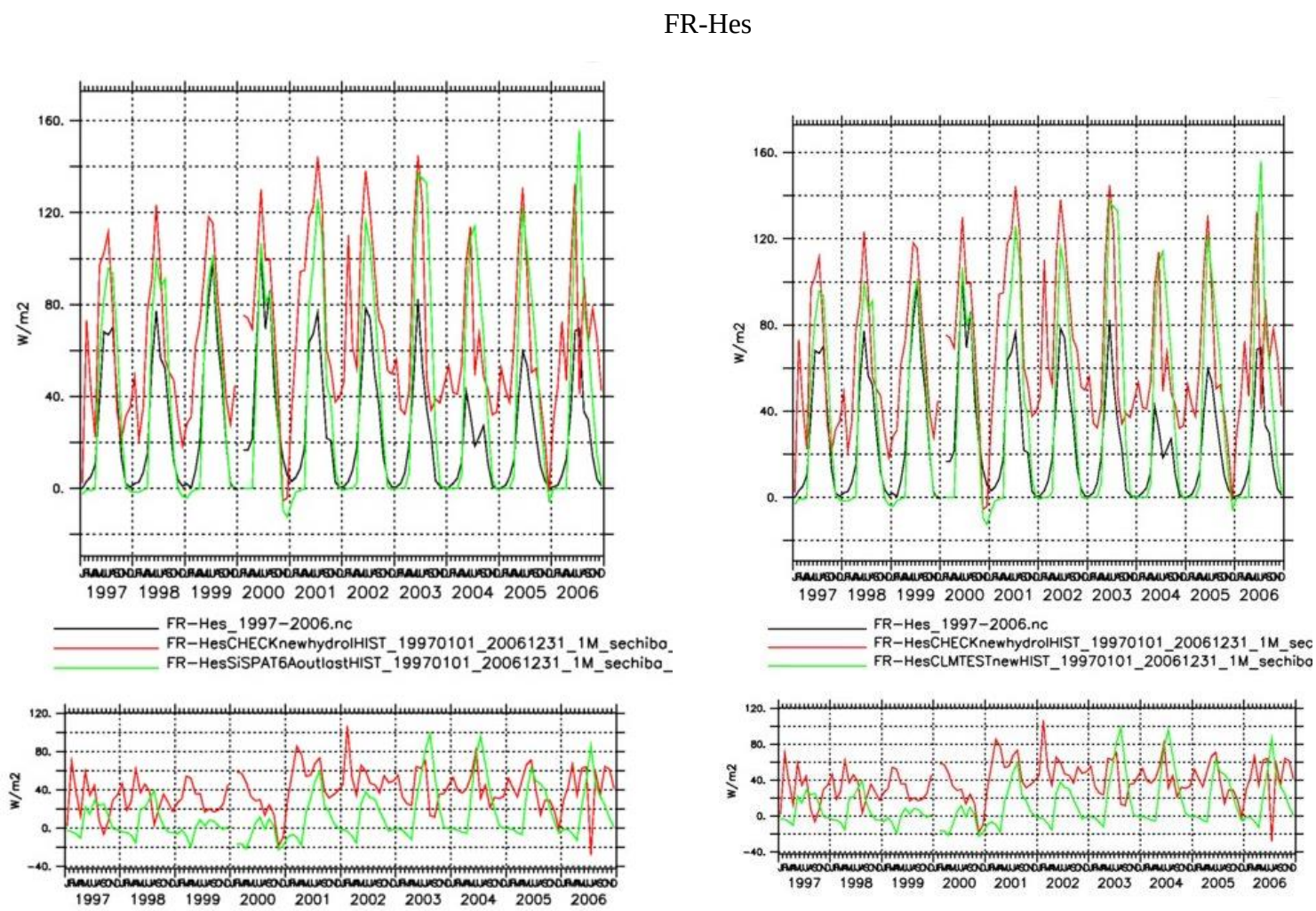

Figure 4-3 Cross validation results of Latent heat flux FR-Hes fluxnet station
left: Based on SiSPAT (Braud, et al., 1995) right: Rootsink activation+Sellers et al. (1992) resistance

US-Var

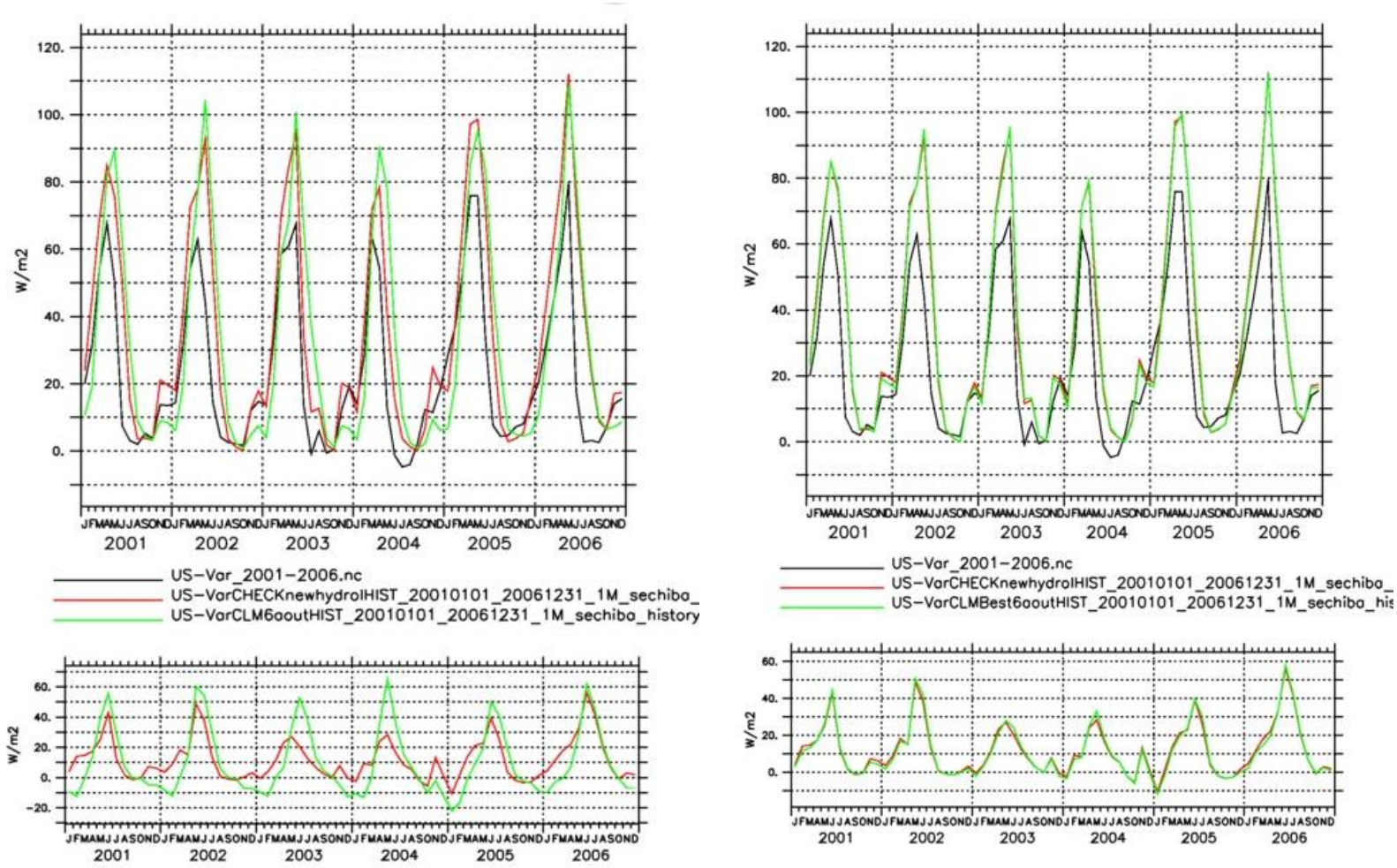

Figure 4-4 Cross validation results of Latent heat flux for US-Var fluxnet station
left: Resistance term by (Sellers, et al., 1992) right: Resistance term by (Best, et al., 2011)

US-Var

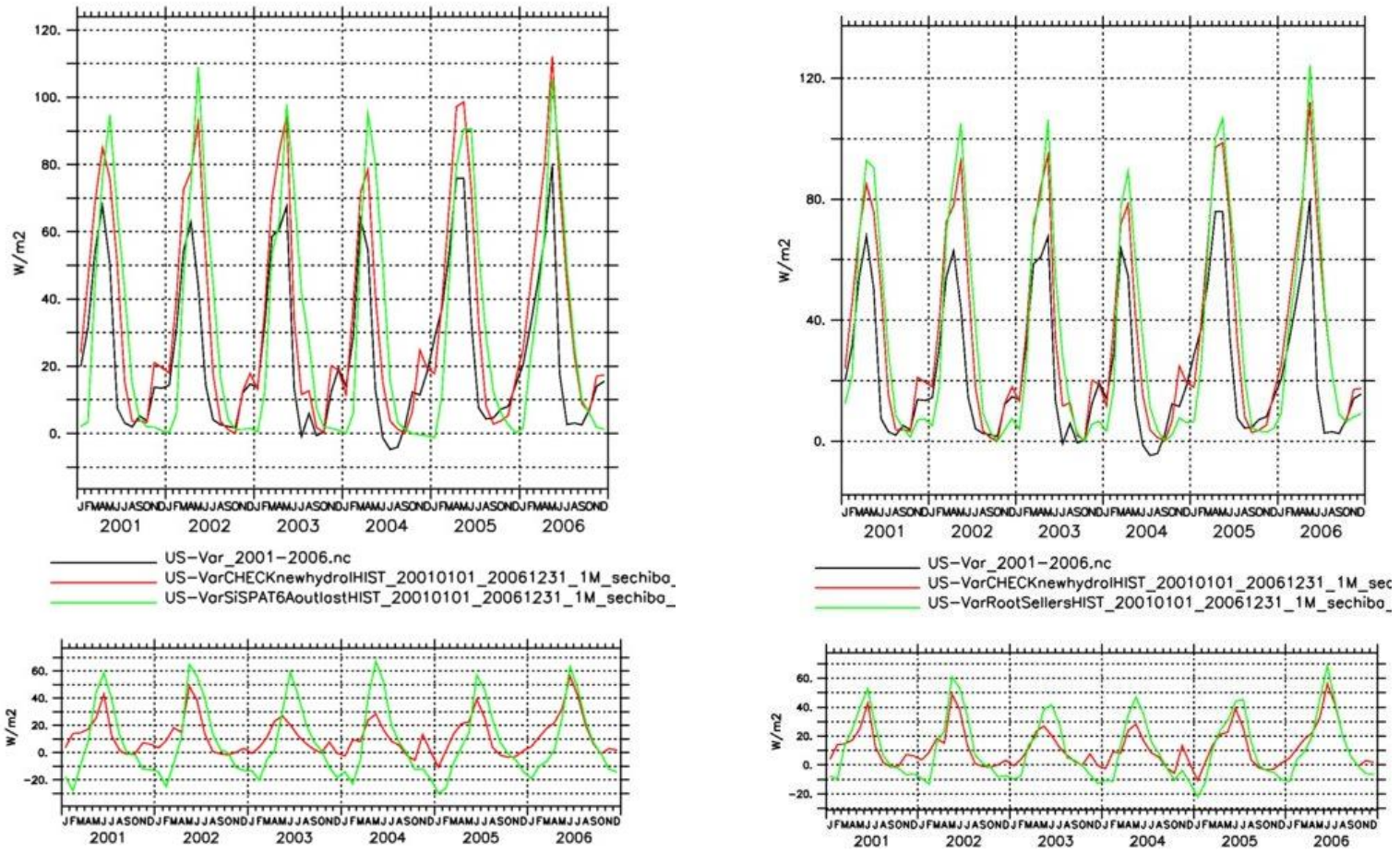

Figure 4-5 Cross validation results of Latent heat flux for US-Var fluxnet station
left: Based on SiSPAT (Braud, et al., 1995) right: Rootsink activation+Sellers et al. (1992) resistance

As it can be noticed in the figures[5], original ORCHIDEE overestimates winter Latent heat flux in deciduous forests to a great extent. While during winters the latent heat flux reaches zero or even negative values, in ORCHIDEE an average overestimation of about 25 $W.m^{-2}$ dominates all years.

In FR-Hes site, almost all four approaches improve the performance and accordance of observed and simulated latent heat, especially during winter, when little latent heat flux is expected because plant transpiration is almost completely stopped. However, in the other site, US-Var (located in a grassland), fluctuation of output is more than reference ORCHIDEE, leading to worse winter underestimation and summer overestimations. This deteriorated performance in US-Var is less significant in the approach which used combination of rootsink activation and soil resistance of Selleres et al. (1992). Figure 4-6, Figure 4-7, Figure 4-8 and show the contribution of each component of total observed latent heat in the three approaches discussed before. The results are discussed in the following three categories; Soil evaporation, Transpiration and Canopy interception:

- Soil evaporation

In FR-Hes which is a deciduous broadleaf forest site, simulations of original ORCHIDEE are overestimating the summer soil evaporation (with fluxes higher than observed latent heat). Among alternative approaches, one using the resistance term by Best et al. (2011) did not significantly improve the performance of the model. Yet winter time soil evaporation is reduced in all three other approaches. Using the SiSPAT formulation for bare soil evaporation led to very low soil evaporation (almost zero).

- Transpiration

In both representative stations summer transpiration is overestimated (more than total observed latent heat). This overestimation is more significant during the second half of summer and at US-Var site. Simulation overestimation is also very important in the last five years of observation at FR-Hes. During the first 5 years, transpiration from plants explains almost all the observed latent heat. But in the years after that (2004 and afterwards), simulated transpiration is almost double the amount of observed latent heat. One possible explanation is the damaging effect of 2003 droughts and heat waves in France on plants and trees which would last several years.

Among different models there is no clear privilege in one or the other, since they all have their advantages and disadvantages.

- Canopy interception

[5] In these figures and also **Error! Reference source not found.**, for each approach, station and variable, two figures are given. The one on top shows the temporal evolution of observed, reference simulation and alternative simulation. The figure on bottom shows the error (distance from observed) of reference and alternative simulation.

Canopy interception does not change in any of the BSE approaches significantly. Since the soil hydraulics are feebly related to the precipitation and surface turbulence, very little change in interception evaporation was expected.

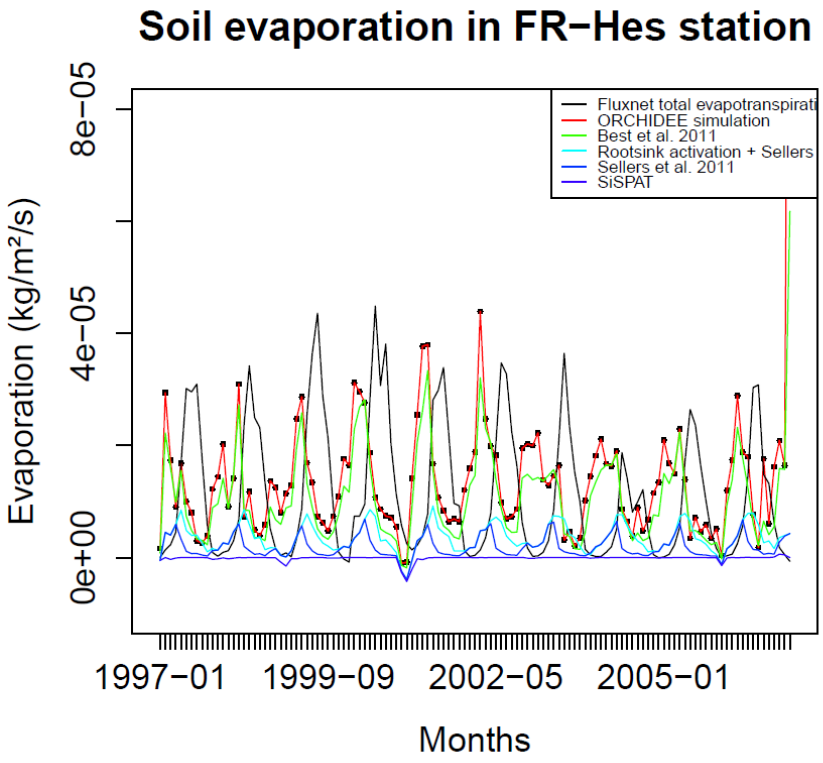

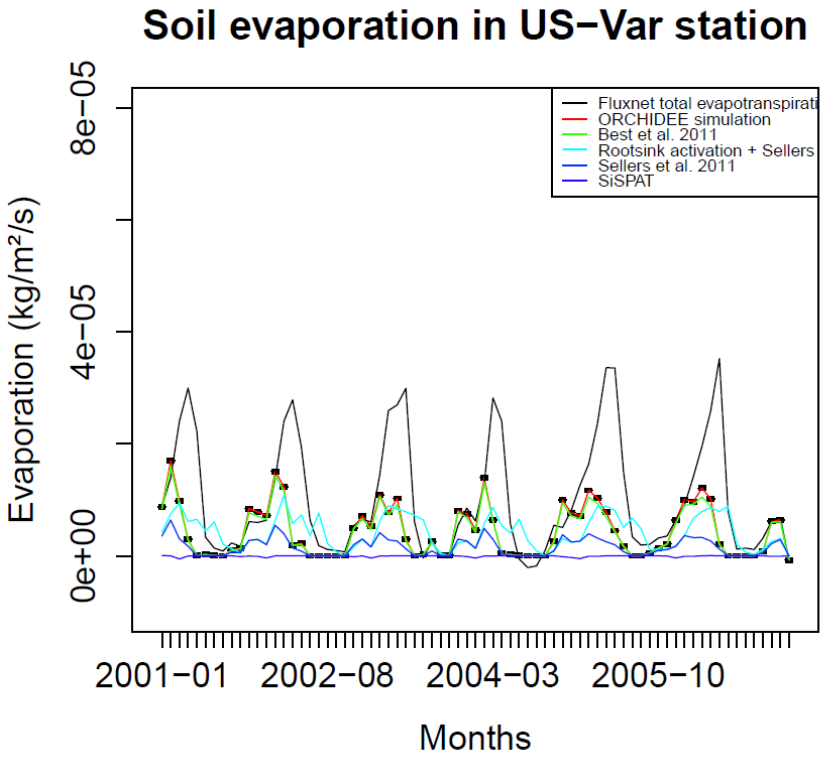

Figure 4-6 Soil evaporation in ORCHIDEE and three alternative simulations versus observed fluxnet latent heat flux

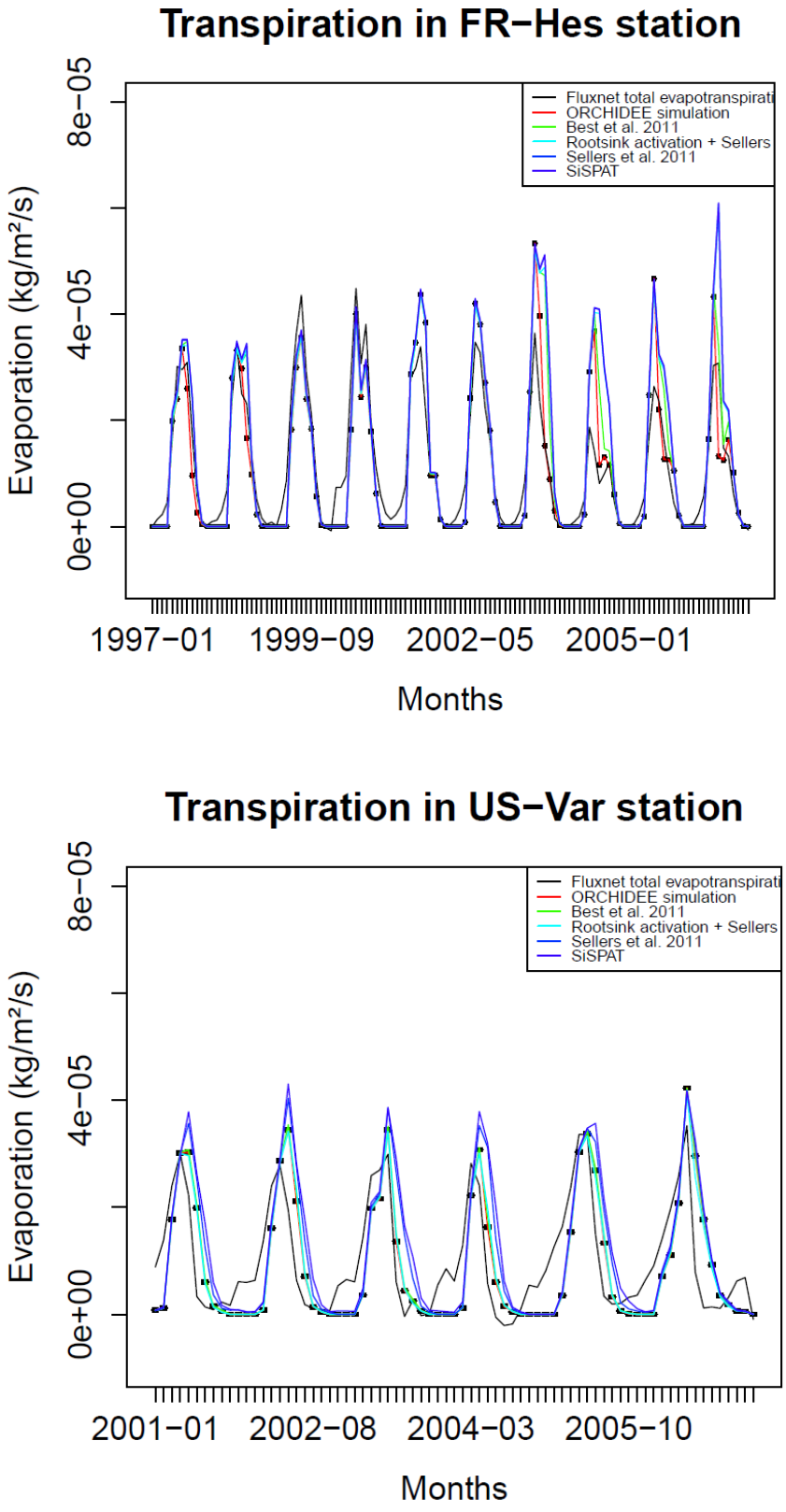

Figure 4-7 Soil evaporation in ORCHIDEE and three alternative simulations versus observed fluxnet latent heat flux

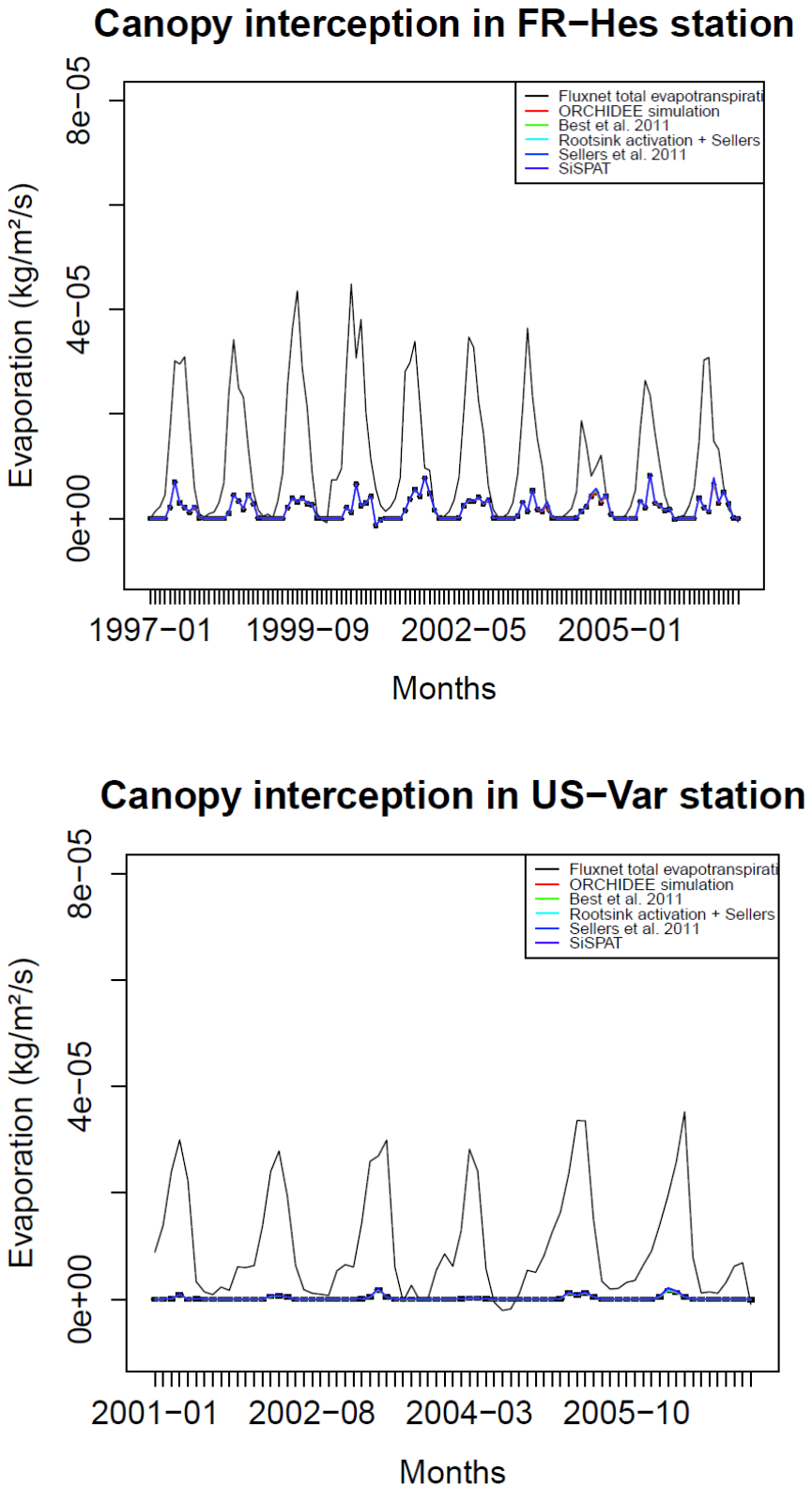

Figure 4-8 Soil evaporation in ORCHIDEE and three alternative simulations versus observed fluxnet latent heat flux

5 Conclusion and perspectives

In the first stage of the study by investigating different methods for calculating evaporation from soil in R software environment and comparing with the deployed method in ORCHIDEE, it is revealed that the later approach is not able to generate enough moderate values of soil evaporation. It means that in ORCHIDEE, either the evaporation demand is met (almost totally), or by using a reducer (a Dirichlet condition) generates the minimum supplied water vapor from soil as evaporation.

In the second step, using ORCHIDEE and a number of formulations and approaches for soil evaporation extracted from technical literature and comparing the results with observed values of latent heat in FLUXNET stations, ORCHIDEE's performance in simulating soil evaporation was assessed. The result showed that using a term of soil resistance or a multiplier h_u (relative humidity) would end in an overall average decrease in soil evaporation but not necessarily affects total evapotranspiration. They would also decrease the frequency of the Dirichlet condition. Among the three approaches for bare soil evaporation calculation, using a resistance term, introduced by Selleres et al (1992), was more successful in correcting the overestimation of latent heat flux in deciduous temperate forests (which was one of the first problems that triggered this study).

Using resistance terms or other methods (using α multiplier or relative humidity in evaporation formulation) resulted in better model performances, especially in regions with broadleaf deciduous forests, where in winter time higher than observed soil evaporation was simulated before. More realistic soil evaporation results in better presentation of latent heat fluxes which would eventually affect plant respiration procedures.

Based on this work, it could be interesting in future studies to investigate the performance of different approaches for bare soil evaporation calculation worldwide, with the use of higher number of reliable FLUXNET stations or global scale and world-wide ET products [Miralles et al, 2011; Jung et al, 2011; Mueller et al, 2013]. Another important issue is to select FLUXNET stations with little energy and flux balance violation. Reliable methods of model performance evaluation in FLEXNET stations with energy balance flaws is the primary step in the validation procedure studies.

It would be of great importance to study soil moisture stress function effect on transpiration and improvement of this function. Long-term effects of severe droughts or heat waves on plant functioning can be the cause of some discrepancies between observed and simulated latent heat, especially during summer. Such extreme climatological conditions can lead to increased root uptake in plants within the following years, reducing soil moisture content to a significant scale.

Appendix

Complementary description of (Brutsaert, 2014)**:**

During the soil controlled evaporation stage, as the upward capillary pressure gradient decreases with increasing depth, at some level it is no longer large enough to drive the water flow upward and the flux is essentially zero. This level defines the lower boundary of the capillary rise layer and it is known as the zero-flux plane, below which water infiltrates downward by the combined driving effects of the pressure gradient and gravity. It is found that while the depth of the zero-flux plane increases gradually as evaporation and infiltration proceed, this increase is likely to be quite limited. If no other information is available, a value of 0.05 d_i would probably be a good first estimate for the depth of the zero-flux plane (0.5d_i-0.66d_i).

The general exact solution yield the evolution of water content distribution in the soil profile with time during the process of evaporation from a bare soil and deeper infiltration following the application of a given amount of precipitation or irrigation. The required parameters for this procedure is the (constant) soil water diffusivity, the (constant) advectivity and the depth of the infiltrating wetting front at the start of the soil-controlled evaporation stage

Complementary table on Aerodynamic resistance

This table is taken from (Katerji, 1977)

Wind speed (m. s^{-1})	Height of vegetation (m)		
	0.2	0.4	0.75
1	120	75	35
2	75	50	20
3	50	35	15
4	38	28	10
5	30	20	9
6	25	17	8

Works Cited

Baldocchi, D. D., Kelliher, F. M., Black, T. A. & Jarvis, P., 2000. Climate and vegetation controls on boreal zone energy exchange. *Global Change Biology,* Volume 6, pp. 69-83.

Baldocchi, D. D. & Meyers, T. P., 1991. Trace gas exchange at the floor of a deciduous forest I. Evaporation and CO2 efflux. *Journal of Geophysical research,* Volume 96, pp. 7271-7285.

Best, M. J. et al., 2011. The joint UK Land Environment Simulator (JULES), model description- Part 1: Energy and water fluxes. *Gesoscientific Model Development,* Volume 4, pp. 677-699.

Blyth, E. et al., 2010. Evaluating the JULES Land Surface Model Energy Fluxes Using FLUXNET Data. *Journal of Hydrometeorology,* Volume 11, pp. 509-519.

Blyth, E. G. et al., 2011. A comprehensive set of benchmark tests for a land surface model of simultaneous fluxes of water and carbon at both the global and seasonal scale. *Gescientific Model Development,* Volume 4, pp. 255-269.

Braud, I., 2000. *SiSPAT a numerical model of water and energy fluxes in the soil plant atmosphere continuum,* Grenoble: CNRS-LTHE.

Braud, I. et al., 1995. A simple soil-plant-atmosphere transfer model (SiSPAT) development and field verification. *Journal of Hydrology,* Volume 166, pp. 213-250.

Brustaert, W., 1982. Evaporation into the atmosphere: Theory, History and applications. In: A. Davenport, et al. eds. Dordrecht: Kluwer Academic Publishers.

Brutsaert, W., 2014. The daily mean zero-flux plane during soil-controlled evaporation: A Green's function approach. *Water Resources Research,* Volume 50, pp. 9405-9413.

Charuchittipan, D. et al., 2014. Extension of the Averaging time in eddy covariance measurements and its effect on the energy balance closure. *Boundary Layer Meterology,* Volume 152, pp. 303-327.

Choudhury, B. J. N. E. D., 1998. A biophysical process-based estimate of glonal land surface evaporation using satellite and ancillary data. I. Model description and comparison with observations. *Journal of Hydrology,* Issue 205, pp. 164-185.

Clapp, R. B. & Hornberger, G. M., 1978. Empirical equations for some soil hydraulic properties. *Water Resources Research,* 14(4), pp. 601-604.

Cosby, B. J., Hornberger, G. M., Clapp, R. B. & Ginn, T. R., 1984. Statistical exploration of the relationships of soil moisture characteristics to the physical properties of soils. *Water Resources Research,* 20(6), pp. 682-690.

d' Orgeval, T., 2006. *Impact du changement climatique sur le cycle de l'eau en Afrique de l'Ouest: Modelisation et incertitudes,* Paris: UPMC.

de Rosnay, P. & Polcher, J., 2002. Impact of a physically based soil water flow and soil-plant interaction representation for modeling large-scale land surface processes. *Journal of Geophysical research,* 107(D11), pp. ACL 3-1-ACL 3-19.

de Rosnay, P. & Polcher, J., 2002. Impact of a physically based soil water flow and soil-plant interaction representation for modeling large-scale land surface processes. *Journal of Geophysical research,* Volume 107, p. D11.

Dirmeyer, P. A. G. X. Z. M. G. Z. O. T. H. N., 2005. *The second global soil wetness project (GSWP-2): Multi Model Analysis and implications for our perception of the land surface,* Tokyo: s.n.

Foken, T., 2008. The Energy Balance Closure Problem: An Overview. *Ecological applications,* Volume 18, pp. 1351-1367.

Jackson, R., 1973. Diurnal changes in soil water content during drying. In: *Field Soil Water Regime.* Madison, Wisconsin: Soil Science Society of America, pp. 37-55.

Jackson, R. D., Kimball, B. A., Reginato, R. J. & Nakayama, F. S., 1973. Diurnal soil water evaporation: Time-depth-flux patterns. *Soil science society of America proceedings,* Issue 37, pp. 505-509.

Jefferson, J. L. & Maxwell, R. M., 2015. Evaluation of simple to complex parametrization of bare ground evaporation. *Journal of advances in modeling earth systesms,* Volume 07.

Jung, M. et al., 2011. Global patterns of land-atmosphere fluxes of carbon dioxide, latent heat, and sensible heat derived from eddy covariance, satellite, and meteorological observation. *Journal of Geophysical Research,* 116(G3).

Katerji, N., 1977. *Contribution a l´etude de l'evapotranspiration reelle du ble tendre d'hiver. Application a la resistance du couvert en relation avec certains facteurs du milieu,* Paris: Universite' Paris 7.

Lawrence, M. D., Thornton, P. E., Oleson, K. W. & Bonan, G. B., 2007. The partitioning of evapotranspiration into transpiration, Soil Evaporation, and Canopy Evaporation in a GCM: Impacts on Land-Atmosphere Interaction. *Journal of Hydrometeorology,* August, Volume 8, pp. 862-879.

Lee, T. J. & Pielke, R. A., 1992. Estimating the soil surface specific humidity. *Journal of Applied Meteorology,* Volume 31, pp. 480-484.

Milly, P. C. D., 1992. Potential evaporation and soil moisture in general circulation models. *Journal of Climate,* Volume 5, pp. 209-226.

Miralles, D. G. et al., 2011. Magnitude and variability of land evaporation and its components at the globale scale. *Hydrology and Earth System Sciences,* Volume 15, pp. 967-981.

Monin, A. S. & Obukhov, A. M., 1954. Basic regularity in turbulent mixing in the surface layer of the atmosphere. *Ak. Nauk, Geof. Inst.,* Volume 24, pp. 163-187.

Moore, K. E., Fitzjerrald, D. R., Sakari, R. K. & Freedman, J. C., 2000. Growing season water balance at a boreal Jack Pine forest. *Water Resources Research,* 36(2), pp. 483-493.

Mueller, B. et al., 2013. Benchmark products for land evapotranspiration: landflux-EVAL multi-data set synthesis. *Hydrology and Earth system sciences,* Volume 17, pp. 3707-3720.

Oleson, K. W. e. a., 2004. *Technical description of the Community Land Model (CLM),* Boulder, Colorado: National Center for Atmospheric Research.

Oleson, K. W. et al., 2008. Improvement to the Community Land Model and their impact on the hydrological cycle. *Journal of Geophysical research,* Volume 113, p. G01021.

Paylin, P. et al., 2015. The ORCHIDEE global land surface model: description and evaluation. *In preparation.*

Reynolds, C. A., Jackson, T. J. & J., R. W., 2000. Estimating soil water-holding capacities by linking the Food and Agriculture Organization soil map of the world with global pedon databases and continuous pedotransfer functions. *Water Resources Research,* 36(12), pp. 3653-3662.

Ringeval, B. et al., 2012. Modelling sub-grid wetland in the ORCHIDEE global land surface model: Evalution against river discharges and remotely sensed data. *Geoscientifuc model development,* Volume 5, pp. 941-962.

Sakaguchi, K. & Zeng, X., 2009. Effects of soil wetness, plant litter, and under-canopy atmospheric stability on ground evaporation in the Community Land Model (CLM3.5). *Journal of Geophysical research,* Volume 114, p. D01107.

Schaap, M. G. & Bouten, W., 1997. Forest floor evaporation in a dense Douglas fir stand. *Journal of Hydrology,* Volume 193, pp. 97-113.

Sellers, P. J., Heiser, M. D. & Hall, F. G., 1992. Relation between surface conductance and spectral vegetation indices at intermediate length scales. *Journal of Geophysical research,* 97(D17), pp. 19033-19059.

Servettaz, A., 2014. *Rapport de stage: Evaluation global du flux d'evapotraspiration simulé par le schéma hydrologique à 11 couches du modèle ORCHIDEE,* Paris: s.n.

Stockli, R. et al., 2008. Use of FLUXNET in the Community Land Model development. *Journal of Geophysical research,* Volume 113, p. G01025.

Stoy, P. C. et al., 2013. A data-driven analysis of energy balance closure across FLUXNET research sites: The role of landscape scale heterofeneity. *Agricultural and Forest Meteorology,* Volume 171-172, pp. 137-152.

Tang, J. Y. & Riley, W. J., 2013. A new top boundary condition for modeling surface diffusive exchange of a generic volatile tracer: Theoretical analysis and application to soil evaporation. *Hydrology and earth system sciences,* Volume 17, pp. 873-893.

Taylor, C. M. & Clark, D. B., 2001. The diurnal cycle and Afrixan easterly waves: A land surface perspective. *Quaterly Journal of the royal meteorological society,* Volume 127, pp. 845-867.

Twine, T. E. et al., 2000. Correcting eddy-covariance flux underestimates over a grassland. *Agricultural and forest meteorology,* Volume 103, pp. 279-300.

Twine, T. E. et al., 2000. Correcting eddy-covariance flux underestimates over a grassland. *Agricultural and Forest Meteorology,* 103(3), pp. 279-300.

van de Griend, A. A. & Owe, M., 1994. Bare soil surface resistance to evaporation by vapor difusion under semi-arid conditions. *Water resources research,* 30(2), pp. 181-188.

Van Genuchten, M., 1980. A closed-form equation for predicting the hydraulic conductivity of unsaturated soils. *Soil Science Society of America Journal,* 44(5), pp. 892-898.

Villegas, J. C., Breshears, D. D., Zou, C. B. & Law, D. J., 2010. Ecohydrological controls of soil evaporation in deciduous drylands: How the hierarchical effects of litter, path and vegetation mosaic cover interact with phenology and season. *Journal of Arid Environments,* 74(5), pp. 595-602.

Wallace, J. S. & Holwill, C. J., 1997. Soil evaporation from tiger-bush in south-west Niger. *Journal of Hydrology,* Volume 188-189, pp. 426-442.

Wilson, K. B., Hanson, P. J. & Baldocchi, D. D., 2000. Factors controlling evaporation and energy partitioning beneath deciduous forest over an annual cycle. *Agricultural and Forest Meteorology,* Volume 102, pp. 83-103.

Wilson, K. et al., 2002. Energy balance closure at FLUXNET sites. *Agricultural and Forest Meteorology,* 113(1-4), pp. 223-243.

Zhang, C., Li, L. & Lockington, D., 2015. A physically based surface resistance model for evaporation from bare soils. *Water resources research,* p. Accepted Article.